**Figure 5** Regulation of miR-222 expression in stellate cells. (A) Expression of miR-221 and miR-222 in mouse stellate cells during primary culture. Isolated mouse stellate cells were cultured for the indicated periods. **p<0.01. PC indicates the expression of miR-221 and miR-222 in isolated mouse hepatocytes. #p<0.01 compared with stellate cells at day 7. (B) Expression of Col1A1 and α-smooth muscle actin (αSMA) mRNAs in mouse stellate cells during primary culture. Glyceraldehyde 3-phosphate dehydrogenase was used as an internal control. *p<0.05, **p<0.01. (C) Expression of miR-221 and miR-221 in HepG2, Huh7, NIH3T3 and LX-2. **p<0.01. (D and E) Regulation of miR-222 expression in mouse primary stellate cells. D: At 1 day after culture, the cells were treated with transforming growth factor α (TGFα; 1 or 10 ng/ml), tumour necrosis factor α (TNFα; 0.1 or 1 ng/ml), or 6-amino-4-(4-phenoxyphenylethylamono) quinazoline (QNZ; 10 or 100 nmol/l) for 24 h. Control indicates non-treated cells. **p<0.01 compared with control. E: At 1 day after culture, the cells were treated with TGFα (1 ng/ml), TNFα (0.1 ng/ml), QNZ (10 nmol/l), TGFα (1 ng/ml) plus QNZ (10 nmol/l), or TNFα (0.1 ng/ml) plus QNZ (10 nmol/l) for 72 h. Control indicates non-treated cells. *p<0.05, **p<0.01. (F) Morphology of mouse stellate cells observed under a microscope (×200) as in (E). (G) Expression of Col1A1 and αSMA mRNAs in mouse stellate cells treated with or without QNZ (10 nmol/l) during primary culture for 72 h.
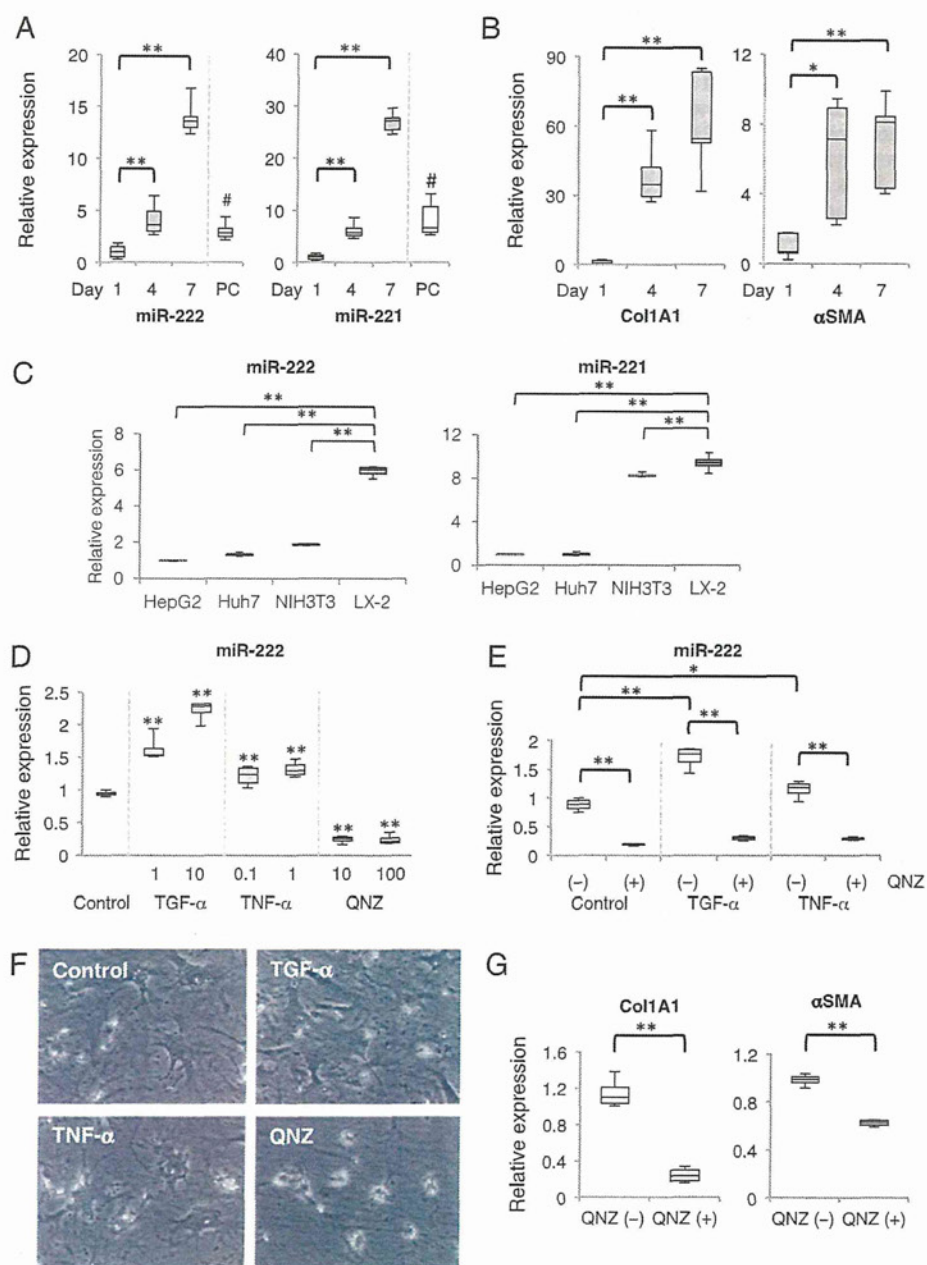

programme in Japan has estimated that the annual incidence of HCC is 0.5–2.0% (mild liver fibrosis; F1/F2) and 5.3–7.9% (advanced liver fibrosis; F3/F4) among patients with chronic hepatitis C.[39] miR-221 and miR-222, a pair of miRNAs encoded in a cluster on chromosome X, are overexpressed in a variety of human cancers, including HCC, in which they play oncogenic roles by downregulating p27, p57 and PTEN expression.[22 37 40] In particular, the pro-tumour activity of miR-221/222 is thought to be achieved by its regulation of CDKN1B (p27, Kip1).[41 42] In this study, we showed that miR-222 interacts with the *CDKN1B* 3'UTR and inhibits the expression of CDKN1B mRNA and protein in LX-2 cells, although it is unclear why increased miR-222 fails to affect the proliferation of stellate cells (figure 6). Type I interferon inhibits the proliferation of LX-2 cells by decreasing cyclin E and increasing p21 without affecting the expression of CDKN1B (p27).[31] In this regard, the

proliferation of stellate cells may be strongly regulated by p21 rather than p27.

In general, miRNAs are transcribed by RNA polymerase II as part of capped and polyadenylated primary transcripts. The primary transcript is cleaved by the Drosha ribonuclease III to generate an approximately 70-nt stem-loop precursor miRNA, which is further cleaved by the cytoplasmic Dicer ribonuclease to generate the mature miRNA. In addition to this common pathway, recent investigations have shown that other factors are involved in the transcription of miRNAs by binding to their promoter regions. For instance, Galardi *et al* identified two separate regions upstream of the miR-221/222 promoter that are bound by the NF-κB subunit p65 and drive efficient transcription in luciferase reporter assays, indicating that the expression of miR-221/222 is induced by NF-κB activation in prostate carcinoma and glioblastoma cells.[33] Because NF-κB is involved in

1607

Hepatology

Figure 6 Interaction of miR-222 with the 3′UTR of CDKN1B mRNA. (A) Schematic indication of the miR-221/222 binding sites in the 3′UTR of CDKN1B mRNA based on TargetScan Human Release 5.1 (http://www.targetscan.org/). Black boxes indicate miR-221 or miR-222. Two predicted target sites of miR-221/222 are present in the 3′UTR of CDKN1B mRNA. (B) Reporter gene assay to test the interaction between the 3′UTR of CDKN1B mRNA and miR-222 in LX-2 cells. Relative luciferase activity derived from pCDKN1B—miR-222/mirGLO in the presence of miR-222 precursors. The pmirGLO vector was used as a negative control reporter vector. NC pre: co-transfection of reporter vectors together with a negative control miRNA precursor, which has a scrambled sequence. miR-222 pre: co-transfection of reporter vectors together with miR-222 precursors. The results are expressed relative to the activity in the presence of negative control precursors. **p<0.01. (C) Effect of miR-222 precursors on the expression of CDKN1B mRNA and protein in LX-2 cells. LX-2 cells were transfected with 50 nM miR-222 precursor (grey column) or a negative control (white column). At 24 h after transfection, CDKN1B mRNA (upper) and protein (lower) were measured. Glyceraldehyde 3-phosphate dehydrogenase (GAPDH) was used as an internal control. **p<0.01. (D) Effect of miR-222 inhibitors on the expression of CDKN1B mRNA and protein in LX-2 cells. LX-2 cells were transfected with 50 nM miR-222 inhibitor (grey column) or a negative control (white column). At 24 h after transfection, CDKN1B mRNA (upper) and protein (lower) were measured. GAPDH was used as an internal control. **p<0.01. (E, F) Effect of 50 nM miR-222 precursors (E) and inhibitors (F) on LX-2 cell growth, determined by WST-1 assay. (G) Effect of miR-222 precursors on the expression of fibrosis-related mRNAs in LX-2 cells. LX-2 cells were transfected with 50 nM miR-222 precursor (grey column) or a negative control (white column). At 24 h after transfection, the mRNAs were quantified. GAPDH was used as an internal control. *p<0.05, **p<0.01. ColA1, α1 (I) collagen; MMP, matrix metalloproteinase; αSMA, α-smooth muscle actin; TGFβ1, transforming growth factor β1; TIMP, tissue inhibitor of matrix metalloproteinase.
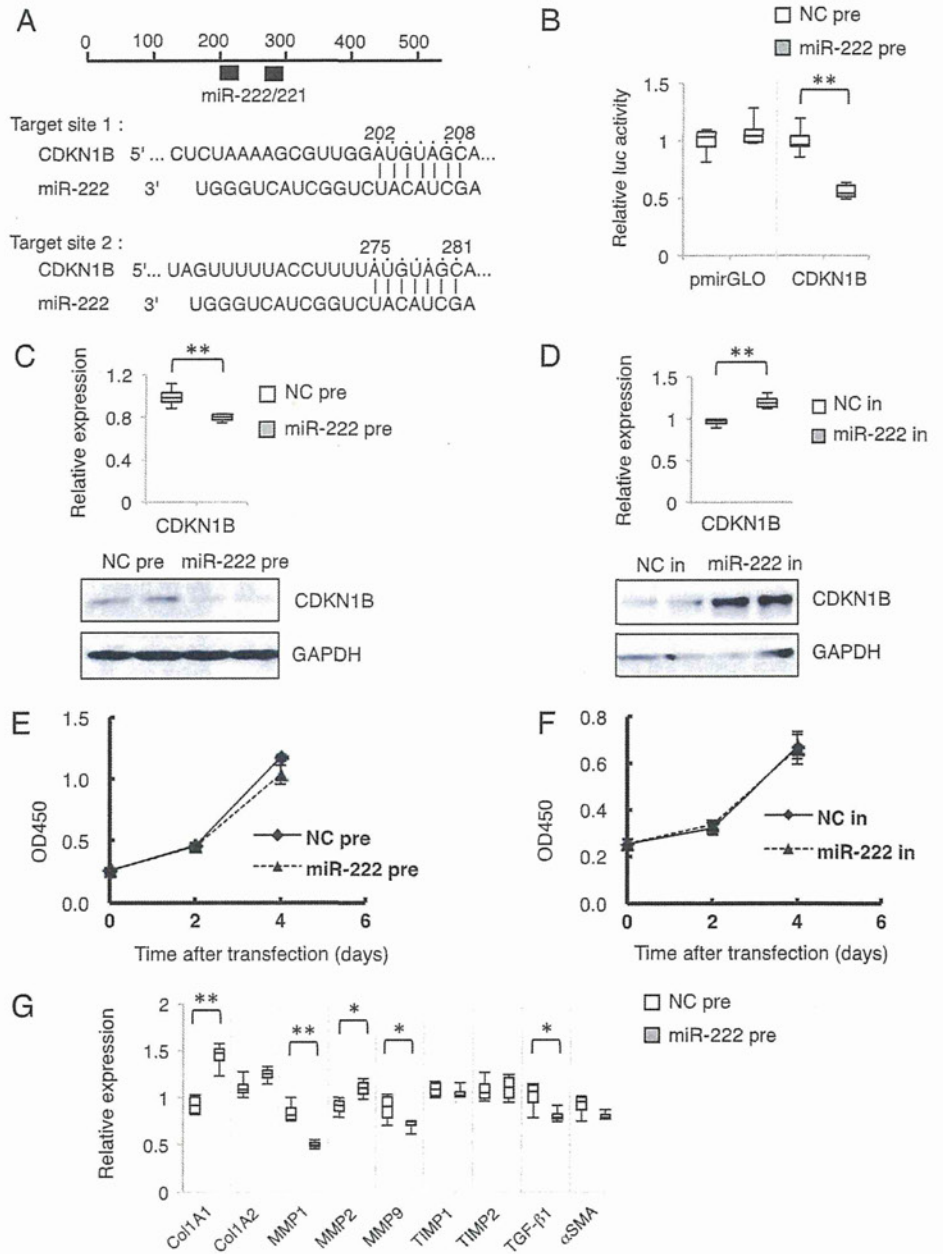
the process of stellate cell activation,[34–36] we speculated that the expression of miR-222 might be regulated through NF-κB activation in stellate cells. We found, however, that miR-222 expression was inhibited by QNZ, an NF-κB inhibitor, accompanied by the morphological maintenance of quiescence, and upregulated by the NF-κB activators TNFα and TGFα.

miRNA expression profiles can serve as useful tools for understanding and investigating the mechanism of the progression of liver fibrosis and can serve as new fibrosis biomarkers. miRNAs are packed into exosomes and circulate in blood.[43] However, this raises the question of whether circulating levels of miRNAs in blood correlate with the progression of liver fibrosis at the tissue level. Roderburg et al demonstrated that the

expression levels of miR-29 family members in human liver fibrosis correlate with the downregulation of miR-29a in the serum.[38] Here, we observed that the expression of miR-222 in human livers with chronic trauma significantly correlated with the expression of Col1A1 mRNA, suggesting that miR-222 is a potential biomarker of liver fibrosis progression, although its utility as a serum biomarker needs further validation. Li et al recently reported that the miR-221 level in blood correlates with cirrhosis, tumour size and tumour stage and provides predictive value for prognosis in patients with HCC.[44]

This study has some limitations. The molecular mechanisms of liver fibrosis in viral hepatitis and in NASH may not exactly the same. In addition, fibrosis in human livers usually progresses

- 183 -

slowly, over the course of decades, so it is not practical to examine the expression of miRNAs at time points throughout progression. In contrast, liver fibrosis in experimental animals progresses quickly, so that within several weeks we could track the changes in miRNA expression at several time points. To establish the utility of miR-221/222 as biomarkers of liver fibrosis irrespective of aetiology, further studies are required to understand the exact mechanism by which the miRNAs participate in the progression of fibrosis.

In conclusion, we showed that miR-221 and miR-222 may be new markers for stellate cell activation and liver fibrosis progression in both humans and mice. These miRNAs could be used in the diagnosis of human liver fibrosis in clinical practice in the near future.

REFERENCES

1. **Friedman SL.** Evolving challenges in hepatic fibrosis. *Nat Rev Gastroenterol Hepatol* 2010;**7**:425—36.
2. **Angulo P.** Nonalcoholic fatty liver disease. *N Engl J Med* 2002;**346**:1221—31.
3. **Matteoni CA,** Younossi ZM, Gramlich T, *et al*. Nonalcoholic fatty liver disease: a spectrum of clinical and pathological severity. *Gastroenterology* 1999;**116**:1413—19.
4. **Brunt EM,** Janney CG, Di Bisceglie AM, *et al*. Nonalcoholic steatohepatitis: a proposal for grading and staging the histological lesions. *Am J Gastroenterol* 1999;**94**:2467—74.
5. **Friedman SL.** Molecular regulation of hepatic fibrosis, an integrated cellular response to tissue injury. *J Biol Chem* 2000;**275**:2247—50.
6. **Kawada N.** Evolution of hepatic fibrosis research. *Hepatol Res* 2011;**41**:199—208.
7. **Wake K.** "Sternzellen" in the liver: perisinusoidal cells with special reference to storage of vitamin A. *Am J Anat* 1971;**132**:429—62.
8. **Filipowicz W,** Bhattacharyya SN, Sonenberg N. Mechanisms of post-transcriptional regulation by microRNAs: are the answers in sight? *Nat Rev Genet* 2008;**9**:102—14.
9. **Bartel DP.** MicroRNAs: genomics, biogenesis, mechanism and function. *Cell* 2004;**116**:281—97.
10. **Brennecke J,** Hipfner DR, Stark A, *et al*. bantam encodes a developmentally regulated microRNA that controls cell proliferation and regulates the proapoptotic gene hid in Drosophila. *Cell* 2003;**113**:25—36.
11. **Schratt GM,** Tuebing F, Nigh EA, *et al*. A brain-specific microRNA regulates dendritic spine development. *Nature* 2006;**439**:283—9.
12. **Chen CZ,** Li L, Lodish HF, *et al*. MicroRNAs modulate hematopoietic lineage differentiation. *Science* 2004;**303**:83—6.
13. **Kota J,** Chivukula RR, O'Donnell KA, *et al*. Therapeutic microRNA delivery suppresses tumorigenesis in a murine liver cancer model. *Cell* 2009;**137**:1005—17.
14. **Chen JF,** Murchison EP, Tang R, *et al*. Targeted deletion of Dicer in the heart leads to dilated cardiomyopathy and heart failure. *Proc Natl Acad Sci U S A* 2008;**105**:2111—16.
15. **Perkins DO,** Jeffries CD, Jarskog LF, *et al*. microRNA expression in the prefrontal cortex of individuals with schizophrenia and schizoaffective disorder. *Genome Biol* 2007;**8**:R27.
16. **Lewis AP,** Jopling CL. Regulation and biological function of the liver-specific miR-122. *Biochem Soc Trans* 2010;**38**:1553—7.
17. **Jopling CL,** Yi M, Lancaster AM, *et al*. Modulation of hepatitis C virus RNA abundance by a liver-specific MicroRNA. *Science* 2005;**309**:1577—81.
18. **Li YP,** Gottwein JM, Scheel TK, *et al*. MicroRNA-122 antagonism against hepatitis C virus genotypes 1-6 and reduced efficacy by host RNA insertion or mutations in the HCV 5' UTR. *Proc Natl Acad Sci U S A* 2011;**108**:4991—6.
19. **Lanford RE,** Hildebrandt-Eriksen ES, Petri A, *et al*. Therapeutic silencing of microRNA-122 in primates with chronic hepatitis C virus infection. *Science* 2010;**327**:198—201.
20. **Pedersen IM,** Cheng G, Wieland S, *et al*. Interferon modulation of cellular microRNAs as an antiviral mechanism. *Nature* 2007;**449**:919—22.
21. **Sarasin-Filipowicz M,** Krol J, Markiewicz I, *et al*. Decreased levels of microRNA miR-122 in individuals with hepatitis C responding poorly to interferon therapy. *Nat Med* 2009;**15**:31—3.
22. **Pineau P,** Volinia S, McJunkin K, *et al*. miR-221 overexpression contributes to liver tumorigenesis. *Proc Natl Acad Sci U S A* 2010;**107**:264—9.
23. **Marquez RT,** Bandyopadhyay S, Wendlandt EB, *et al*. Correlation between microRNA expression levels and clinical parameters associated with chronic hepatitis C viral infection in humans. *Lab Invest* 2010;**90**:1727—36.
24. **Bedossa P,** Poynard T. An algorithm for the grading of activity in chronic hepatitis C. The METAVIR Cooperative Study Group. *Hepatology* 1996;**24**:289—93.
25. **Sato F,** Tsuchiya S, Terasawa K, *et al*. Intra-platform repeatability and inter-platform comparability of microRNA microarray technology. *PLoS One* 2009;**4**:e5540.
26. **Ikejima K,** Honda H, Yoshikawa M, *et al*. Leptin augments inflammatory and profibrogenic responses in the murine liver induced by hepatotoxic chemicals. *Hepatology* 2001;**34**:288—97.
27. **Mu YP,** Ogawa T, Kawada N. Reversibility of fibrosis, inflammation and endoplasmic reticulum stress in the liver of rats fed a methionine-choline-deficient diet. *Lab Invest* 2010;**90**:245—56.
28. **Kristensen DB,** Kawada N, Imamura K, *et al*. Proteome analysis of rat hepatic stellate cells. *Hepatology* 2000;**32**:268—77.
29. **Xu L,** Hui AY, Albanis E, *et al*. Human hepatic stellate cell lines, LX-1 and LX-2: new tools for analysis of hepatic fibrosis. *Gut* 2005;**54**:142—51.
30. **Ogawa T,** Iizuka M, Sekiya Y, *et al*. Suppression of type I collagen production by microRNA-29b in cultured human stellate cells. *Biochem Biophys Res Commun* 2010;**391**:316—21.
31. **Sekiya Y,** Ogawa T, Iizuka M, *et al*. Down-regulation of cyclin E1 expression by microRNA-195 accounts for interferon-beta-induced inhibition of hepatic stellate cell proliferation. *J Cell Physiol* 2011;**226**:2535—42.
32. **Murakami Y,** Toyoda H, Tanaka M, *et al*. The progression of liver fibrosis is related with overexpression of the miR-199 and 200 families. *PLoS One* 2011;**6**:e16081.
33. **Galardi S,** Mercatelli N, Farace MG, *et al*. NF-kB and c-Jun induce the expression of the oncogenic miR-221 and miR-222 in prostate carcinoma and glioblastoma cells. *Nucleic Acids Res* 2011;**39**:3892—902.
34. **Lee KS,** Buck M, Houglum K, *et al*. Activation of hepatic stellate cells by TGF alpha and collagen type I is mediated by oxidative stress through c-myb expression. *J Clin Invest* 1995;**96**:2461—8.
35. **Rippe RA,** Schrum LW, Stefanovic B, *et al*. NF-kappaB inhibits expression of the alpha1(I) collagen gene. *DNA Cell Biol* 1999;**18**:751—61.
36. **Lang A,** Schoonhoven R, Tuvia S, *et al*. Nuclear factor kappaB in proliferation, activation and apoptosis in rat hepatic stellate cells. *J Hepatol* 2000;**33**:49—58.
37. **Fornari F,** Gramantieri L, Ferracin M, *et al*. MiR-221 controls CDKN1C/p57 and CDKN1B/p27 expression in human hepatocellular carcinoma. *Oncogene* 2008;**27**:5651—61.
38. **Roderburg C,** Urban GW, Bettermann K, *et al*. Micro-RNA profiling reveals a role for miR-29 in human and murine liver fibrosis. *Hepatology* 2011;**53**:209—18.
39. **Yoshida H,** Shiratori Y, Moriyama M, *et al*. Interferon therapy reduces the risk for hepatocellular carcinoma: national surveillance program of cirrhotic and noncirrhotic patients with chronic hepatitis C in Japan. IHIT Study Group. Inhibition of Hepatocarcinogenesis by Interferon Therapy. *Ann Intern Med* 1999;**131**:174—81.
40. **Garofalo M,** Di Leva G, Romano G, *et al*. miR-221&222 regulate TRAIL resistance and enhance tumorigenicity through PTEN and TIMP3 downregulation. *Cancer Cell* 2009;**16**:498—509.
41. **Ie Sage C,** Nagel R, Egan DA, *et al*. Regulation of the p27(Kip1) tumor suppressor by miR-221 and miR-222 promotes cancer cell proliferation. *Embo J* 2007;**26**:3699—708.
42. **Galardi S,** Mercatelli N, Giorda E, *et al*. miR-221 and miR-222 expression affects the proliferation potential of human prostate carcinoma cell lines by targeting p27Kip1. *J Biol Chem* 2007;**282**:23716—24.
43. **Kosaka N,** Iguchi H, Ochiya T. Circulating microRNA in body fluid: a new potential biomarker for cancer diagnosis and prognosis. *Cancer Sci* 2010;**101**:2087—92.
44. **Li J,** Wang Y, Yu W, *et al*. Expression of serum miR-221 in human hepatocellular carcinoma and its prognostic significance. *Biochem Biophys Res Commun* 2011;**406**:70—3.

MicroRNA-221/222 upregulation indicates the activation of stellate cells and the progression of liver fibrosis

Tomohiro Ogawa, Masaru Enomoto, Hideki Fujii, et al.

Updated information and services can be found at:
http://gut.bmj.com/content/61/11/1600.full.html

These include:

References	This article cites 44 articles, 10 of which can be accessed free at: http://gut.bmj.com/content/61/11/1600.full.html#ref-list-1
Email alerting service	Receive free email alerts when new articles cite this article. Sign up in the box at the top right corner of the online article.

Topic Collections	Articles on similar topics can be found in the following collections Cirrhosis (266 articles) Hepatic cancer (364 articles)

Notes

Mice with Liver Composed of Human Hepatocytes as an Animal Model for Drug Testing

Katsutoshi Yoshizato[1,2,*], Chise Tateno[1], and Rie Utoh[3]

[1]*Phoenixbio Co., Ltd, Hiroshima, Japan;* [2]*Liver Research Center and Synthetic Biology Laboratory, Osaka City University Graduate School of Medicine, Osaka, Japan and* [3]*The Institute of Advanced Biomedical Engineering and Science, Tokyo Women's Medical University, Tokyo, Japan*

Abstract: Conventionally, rodents, mostly mice and rats, have been utilized as animal models for studying drug metabolism and toxicity of new medicines. However, there have been two major problems inherent to these models. One is that there are species differences in major enzymes responsible for drug metabolisms and detoxification such as cytochrome P450 between rodents and humans, and the other is that human hepatitis viruses do not infect rodent livers, which hampers studies for anti-hepatitis virus drugs using these models. As an approach to overcome these intrinsic shortages, we devised a method to generate mice whose livers are mostly (>80%) repopulated with healthy human hepatocytes 7 years ago. Since then, these mice called simply chimeric mice or liver-humanized mice have been widely utilized among researchers in the areas for new drug developments, which, as a result, have proved that the chimeric mouse is a practical solution to solve the above two issues. The hitherto accumulated studies demonstrating the similarities of the chimeric mouse liver to the human crude liver are summarized and reviewed in the present article. In addition, there have been also studies that show us the presence of dissimilarities between them, such as human hepatocytes' manifestation of hyperplasia in mouse liver and their steatotic alterations when the mice are maintained for >50 days post-transplantation. These dissimilarities between them are also reviewed in details, considering that the information of the similarities and the dissimilarities is quite useful to researchers who utilize chimeric mice as a drug discovery tool for correctly evaluating the obtained results.

Keyword: Growth hormone, hepatic stellate cells, hepatitis viruses, *in vivo* drug testing, liver regeneration, liver steatosis, Mice with human liver, TGF-β signaling.

INTRODUCTION

Science is the activity to understand a phenomenon of interest by knowing the relationships among the components that are included in a phenomenon. Usually, we are able to directly collect samples from entities that participate in a phenomenon and analyze the samples. However, samples from humans are generally hard to be collected even in the case of diseased persons, *i.e.* normal and healthy human samples are practically inaccessible except the cases in which test samples are considered to be indispensable to cure diseases. Rare healthy samples collected under exceptionally acceptable conditions are thus highly precious for revealing the biological and physiological features of human tissues and cells. As a matter of fact *in vivo* experimentation with humans to understand their normal processes of biological and physiological phenomena is impossible, contrasting with relative easiness of non-human vertebrates and free accessibility of non-vertebrates for the scientific purposes.

Conventionally, rodents, especially mice and rats, have been utilized as animal models for studies that aim to understand human biology and pathology in spite of the presence of species differences in many aspects of biological features between humans and rodents. Under these situations one possible approach for revealing *in vivo* features of human tissues and cells has been to create a rodent that bears human tissues/cells. A major target organ for studying drug metabolism and toxicity in R&D areas of new medicines is liver, because its parenchymal cells, principally hepatocytes, play prime roles in drug metabolisms and detoxifications [1, 2]. Therefore, creation of a liver-chimeric rodent, a rodent whose hepatocytes in liver are humanized by being replaced with human (h) hepatocytes (*h*-hepatocytes), might greatly contribute to R&D studies of drug development. Conventionally, mice have been preferred to rats, because their genetic data are richer and gene technology is applicable more easily in the former.

Hepatocyte-humanized mice were created as a suitable animal model for studying infection and propagation of hepatitis viruses (HVs) by using severe combined immunodeficient (SCID) mice as hosts that carry albumin (Alb)-promoter/enhancer-driven urokinase-type plasminogen activator (uPA) gene [3, 4]. As expected hepatitis viruses B and C (HBV and HCV) infected their livers as the liver in human body when the mice were injected with sera from HBV/HCV patients, which in turn provided us a piece of evidence for actual humanization of the mouse liver. Since then the chimeric mice have been thought to be an ideal animal model

*Address correspondence to this author at the Phoenixbio Co. Ltd., 3-4-1-Kagamiyama, Higashi, Hiroshima, Japan; Tel: +81-82-431-0016; Fax: +81-82-431-0017; Email: katsutoshi.yoshizato@phoenixbio.co.jp

for investigating mechanism of infection of these viruses and their proliferation therein and also to be quite useful test animals for discovery and characterization of anti HCV/HBV drugs [5].

Usefulness of chimeric mice as experimental tool depends on the extent of replacement of host hepatocytes with transplanted *h*-hepatocytes, because the presence of residual mouse (m)-hepatocytes (*m*-hepatocytes) hinders researchers from determining correct phenotypes of *h*-hepatocytes and would even affect the functions and activities of *h*-hepatocytes. It is clear that generation of chimeric mice whose livers are composed of mostly *h*-hepatocytes is especially vital to testing for metabolism and detoxification of drugs. Mice completely replaced with *h*-hepatocytes would be ideal, which, however, have not been attainable yet up to now in a reproducible manner. The extent of *h*-hepatocyte replacement is practically estimated by measuring concentrations of human Alb (hAlb) in host blood using human-specific antibodies or, when necessary, is correctly determined immunohistochemically as the number ratio [replacement index (RI)] of *h*-hepatocytes to total *h*- and *m*-hepatocytes using hepatocyte-specific proteins such as cytokeratin (CK) 8/18 as antigens. Liver sections are stained with the corresponding human-specific antibodies. The ratio of immuno-positive to examined entire area represents RI. We first developed methods and technologies to reproducibly produce chimeric mice with RI >70% using homogeneous populations of *h*-hepatocytes derived from individual donors [6]. Utilizing such chimeric mice with high RIs we were able to demonstrate that chimeric livers showed expression profiles of genes and proteins of major members of cytochrome P450 (CYP) similar to those of hepatocyte donors in a drug-dependent manner, strongly supporting our expectation that chimeric mice could be utilized as a useful animal model for predicting human metabolic profiles of test drugs [6]. The original methodology of chimeric mouse production has further been improved to a level of mass-production of homogenous chimeric mice with RI = ~90%, which enabled us to industrialize chimeric mice for drug testing [7, 8].

"Ready for use"-type availability of reproducible high-RI chimeric mice accelerated their detailed characterization with respect to propagation of *h*-hepatocytes, hepatic architectures, profiles of CYPs against various drugs (Phase I pathways), conjugation pathways (Phase II), and transports of known drugs, and infection and proliferation of HCV/HBV [7, 8]. Repopulation processes of *h*-hepatocytes in the damaged host liver were also investigated focusing on epitheliomesenchymal interactions between *h*-parenchymal cells and mouse non-parenchymal cells [9]. Recently, we reported an endocrinological problem inherent to chimeric mouse liver: *h*-hepatocytes were found to be growth hormone (GH)-deficient because the cells are indifferent to mouse GH, which causes *h*-hepatocyte lipogenesis [10].

Since we started on a task to provide researchers for drug R&D and those studying HCV/HBV infection mechanisms with *h*-chimeric mice with high RIs, ~7 years have passed. Collectively, hitherto accumulated data have proved that the chimeric mouse is appreciably humanized in the metabolic profiles of known drugs and HCV/HBV infection mecha-
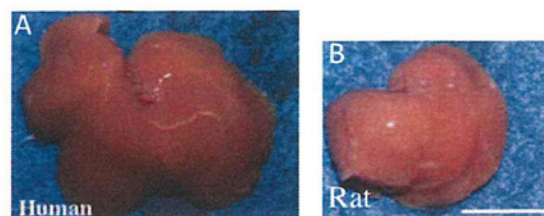

Fig. (1). Representative gross appearance of livers from *h*- and *r*-hepatocyte chimeric mice. *h*- and *r*-chimeric mice were generated by transplanting hepatocytes from a 9-year-old boy (**A**) and a 13-week-old male Fisher 344 rat (**B**). The *h*- and *r*-chimeric mice were killed 90 and 100 days post-transplantation, respectively their livers were photographed and analyzed for determining RIs and the ratios ($R_{L/B}$) of liver weight against body weight. The RI for the *h*- and *r*-chimeric mouse was 92 and 100%, respectively and $R_{L/B}$ 19.3 and 6.5%, respectively. Bar represents 1 cm. The photos are cited from the literature No. 9.

nisms in spite of the fact that the nonparenchymal tissues of the liver are totally composed of mouse cells and extracellular matrices. Thus, interests in chimeric mouse are increasing as a test animal model for predicting metabolic profiles of general and anti HCV/HBV drugs in pharmaceutical areas. We have had opportunities to review *h*-chimeric mouse studies emphasizing the "similarity" of *h*-hepatocyte characteristics between human liver and *h*-chimeric mouse livers [7, 8]. The present article aims to review present status of chimeric mouse studies emphasizing the "dissimilarity" of *h*-hepatocytes between the two livers with respect of hepatic architechtures, *h*-hepatocyte growth capacity, hepatocyte-nonparenchymal cell interactions, and endocrinological features and lipid metabolisms.

TISSUE ARCHITECTURES OF CHIMERIC MOUSE LIVER

The success in generating hepatocyte-humanized mice itself indicates that both donor hepatocytes and host nonparenchymal tissues could reconcile each other and manage well to reconstruct the chimeric liver. To measure the difficulty (easiness) of this reconciliation and management, we compared the chimerism by *h*- and rat (*r*) hepatocytes generated by transplanting *h*- and *r*-hepatocytes in uPA/SCID mice under the same conditions [9]. The obtained results clearly showed the much easiness in producing rat chimerism compared to human chimerism. First, repopulation speed of *h*-hepatocytes (~8% replacement/week) was much slower than that of *r*-hepatocytes (~30%/week). *h*-Hepatocytes require approximately four times longer time of periods to complete repopulation than *r*-hepatocytes. Second, *r*-hepatocyte repopulation was terminated with the complete repopulation (RI = 100%) at 3 weeks after transplantation, but that of *h*-hepatocytes was terminated with incomplete repopulation (~70% in average) even at 8 weeks posttransplantaion. Livers of *h*-hepatocyte and *r*-hepatocyte chimeric mice (RI = 94 and 100% for the former and latter, respectively) both looked macroscopically normal and healthy except that the former (Fig. 1A) was quite bigger in volume than the latter (Fig. 1B). Semi-macroscopic views of each of six among seven liver lobules are shown in (Fig. 2A), which was obtained from a chimeric mouse that had been transplanted with 10^6 hepatocytes from a 6-year-old girl. The
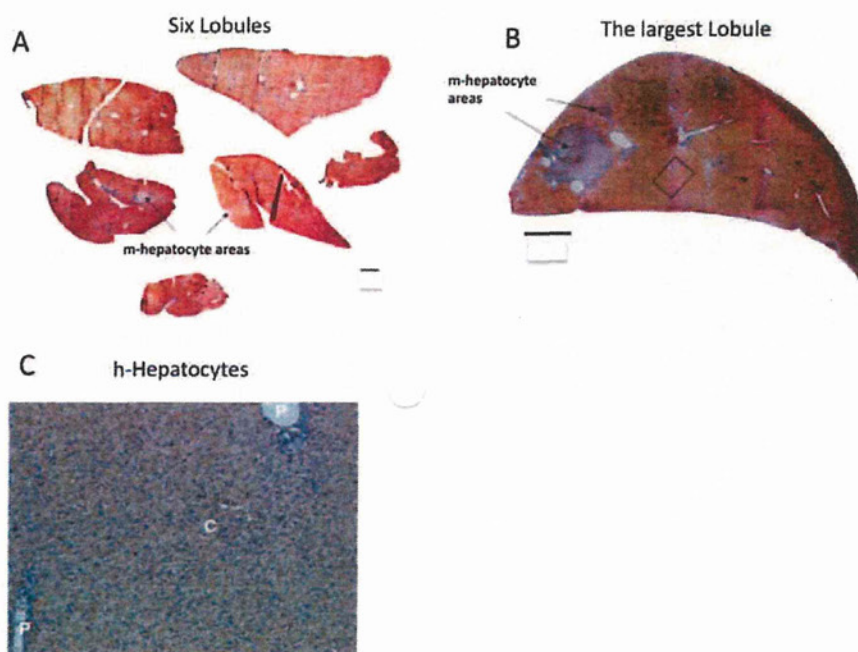
Fig. (2). Semi-macroscopic views of *h*-chimeric mouse lobules. *h*-Chimeric mice were produced with hepatocytes from a 6-year-old girl (**A**) and a 9-month-old boy (**B**). The rectangular area indicated in B was enlarged in C. See detailed explanations of the photos in the text. Bars in A, B, and C represent 1 µm, 1 µm and 100 mm, respectively. P and C in C indicate the location of portal and central veins, respectively. The photos are cited from the literature No. 8.

mouse in this case was sacrificed 77 days post-transplantation and its six liver lobules were sectioned for h-CK8/18 staining to locate *h*-hepatocyte regions. RI reached as high as ~99%. Quite small *m*-hepatocytic regions were present as indicated by arrows. A similar view of the largest lobule is shown in (Fig. **2B**) obtained from a chimeric mouse with RI = 82% that had been transplanted with 7.5 x 10^5 9-month-old boy's hepatocytes and killed at 80 days after transplantation. Its histology shows the well organized architectures of hepatic plates consisting of *h*-hepatocytes and *m*-nonparenchymal cells with the well-developed sinusoidal streams between portal and central veins (Fig. **2C**).

Hepatocytes are the parenchymal cells of the liver that pursuit "liver function". The hepatic nonparenchyma contains several species of cells such as sinusoidal endotherial cells, stellate cells and Kupffer cells. These cells aggregate and construct the liver with following number ratios, hepatocytes:Kupffer cells:stellate cells:endothelial cells = 52: 18: 8: 22 (%) in the case of mouse [11]. Hepatocytes are closely apposed in an orderly fashion and concentrate in a structurally stable mass called the hepatic plate by direct intercellular adhesions, which are structurally connected with nonparenchymal cells, forming liver-specific unique architectures including sinusoids where liver cells such as hepatocytes, stellate cells, Kupffer cells, and capillary cells communicate each other (Fig. **3**) [12]. The Kupffer cell and the pit cell (NK cell) rest on the fenestrated endothelial cell that contacts the poorly developed basement membrane of the sinusoid. A unique structure is formed between the hepatocyte plate and the sinusoidal basement membrane, which is defined as the space of Disse. The stellate cell, storing vitamin A in the lipid droplets, is located in this space, extending interhepato-
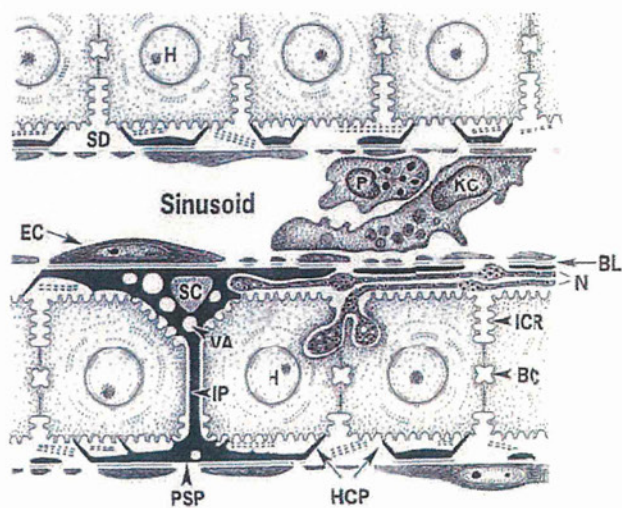

Fig. (3). Histological organization of mammalian liver tissue by hepatocytes and nonparenchymal liver cells. The tissue organization is schematically drawn focusing on the sinusoidal wall. The Kupffer cell (KC) and the pit cell (P) rest on the fenestrated endothelial cell (EC), which in turn contacts the hepatic stellate cell (SC) with poorly-developed basement membrane (BL) between both cells. The stellate cell, storing vitamin A in the lipid droplets (VA), extends interhepatocellular processes (IP) and perisinusoidal, or subendothelial processes (PSP), which encompass the endothelial tube. The stellate cells contact the hepatocyes (H) with their thorn-like microprojections or hepatocyte-contacting processes (HCP). The space between the endohelial cell-stellate cell complex and the hepatocyte is defined as the space of Disse (SD). Collagen fibrils and nerve fibers (N) course through the space of Disse. BC, bile canaliculus; ICR, interhepatocellular recess. This illustration is cited from the literature No. 12.
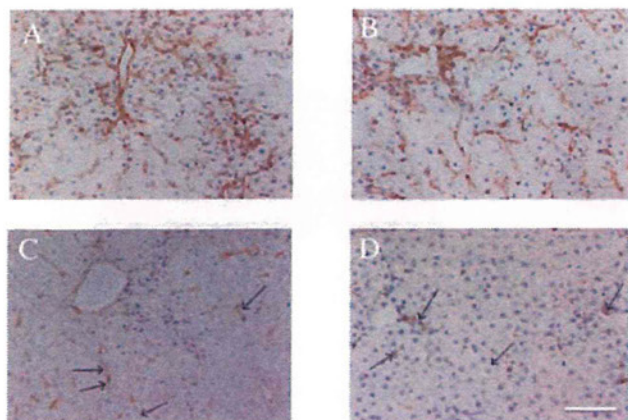
Fig. (4). Construction of chimeric liver by *h*-hepatocytes in association with *m*-nonparenchymal cells. uPA/SCID mice were transplanted with *h*-hepatocytes and allowed to grow until the repopulation of the liver was complete when the hosts were killed for examining histological features by immunohistological techniques. Sections were immunostained with antibodies for type IV collagen (**A**), laminin (**B**), stabillin (**C**), a marker of liver endothelial cells (a gift from Dr. A. Miyajima, Tokyo University), and BM8 (**D**), a marker of Kupffer cells. The immunosignals are brown. The arrows in (**C**) and (**D**) point to typical immunopositive cells. Bar represents 100 μm. These photos are cited from the literature No. 7.
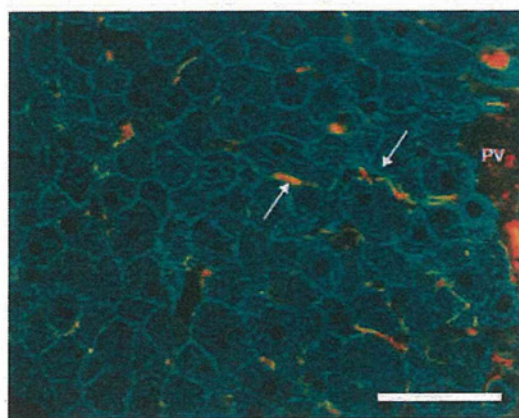

Fig. (5). Chimeric sinusoids formed by the elaborate collaboration of *h*-hepatocytes with *m*-nonparenchymal cells. A chimeric mouse was generated by transplanting 6-year-old girl's hepatocytes and killed 90 days posttransplantation when RI was ~80% for double-immunohistologically locating *h*-hepatocytes and *m*-hepatic stellate cells using antibodies against h-CK8/18 and desmin, respectively. *h*-Hepatocytes are stained green and *m*-stellate cells red. Arrows point to *m*-stellate cells. PV: portal vein. Bar represents 50 μm. This photo is sited from the literature No. 8.

cellular processes and perisinusoidal, or subendothelial processes, which encompass the endothelial tube. The stellate cells contact the hepatocyes with their thorn-like microprojections or hepatocyte-contacting processes. Collagen fibrils and nerve fibers course through the space of Disse.

Macro- and semi-macroscopical examinations shown in Figs. (**1** and **2**) suggest that *h*-hepatocytes normally communicate with *m*-nonparenchymal cells as *m*-hepatocytes do, which was supported by a study in which distributions of *h*-

hepatocytes and *m*-stellate cells were examined by double-immunohistology on chimeric liver using animal species- and cell type-specific antibodies against CK8/18 for *h*-hepatocytes and desmin for *m*-stellate cells (Fig. **4**). *h*-Hepatocytes appear to be normally associated with *m*-stellate cells along the sinusoidal capillaries. Livers of *h*-chimeric mice with RI >70% were further examined to know normality/abnormality of the architectures constructed by *h*-hepatocytes, host nonparenchymal cells and host extracellular matrices (ECMs) using antibodies against type IV, laminin, stabilin for liver endothelial cells, BM8 for Kupffer cells, desmin for stellate cells, and human specific CK8/18 for hepatocytes. At glance these staining patterns first show a close association of *h*-hepatocytes with host nonparenchymal cells and second an apparent normal development of vascular systems with hepatic sinusoids (Fig. **5**).

The liver enlargement was only a macroscopic abnormality we noticed. To examine this phenomenon at the microscopical level, we made a detailed histological survey on sinusoidal architectures comparing to those of *r*-hepatocyte chimeric liver [9], because firstly rats are phyrogenetically quite close to mice and secondly it was shown that *r*-hepatocytes completely repopulate the liver of uPA/SCID mouse without any visible abnormal symptons [13]. Particularly we paid attention to the structures of hepatic plates and sinusoids, because they reflects the proliferation status of hepatocytes, *i.e.*, the hepatic plates are of single-cell layer and sinusoidal structures are compressed when hepatocytes are in non-proliferative (resting) conditions [14], but the former become multicell-layer thick and the latter become vague during vigorous hepatocyte proliferation [15]. *r*- and *h*-Hepatocyte chimeric mice were generated by transplanting hepatocytes from 13-week-old male Fisher 344 rats and a 9-month-old-male donor, respectively. They were sacrificed in the proliferation phase (P-phase) and the proliferation termination phase (T-phase). In the case of *r*-hepatocyte (*r*-hep) chimeric mice, the mice were killed at 2 weeks post-transplantation when the *r*-hepatocytes were in P-phase and RI was ~55%, and at 5 weeks when they were in T-phase and RI was100%. In the case of *h*-hepatocyte chimeric mice, the mice were killed at 5 weeks post-transplantation when the *h*-hepatocytes were in P-phase and RI was ~30%, and at 14 weeks when they were in T-phase and RI was ~70%. Their livers were subjected to investigating distributions of type IV collagen for sinusoidal spaces, multidrug resistance-associated protein (MRP2) for canalicular organic anion transporters (Fig. **6** and **7**). Normal livers from both human and rat specimens show the single-cell structures of hepatic plates on hematoxylin and eosin (H&E) sections (Fig. **6A** and Fig. **7A**, respectively). As we expected, both *h*- and *r*-hepatocyte chimeric livers at P-phase do not show such single-cell plates, but show multicell-layer-thick hepatic plates (Fig. **7D** for rat liver and data not shown for human liver). The MRP2 protein is randomly distributed in the intercellular space in P-phase (Fig. **7E** for rat liver and data not shown for human liver), sinusoidal structures are also not in an orderly fashion, losing vessel continuity along the portal-central axis. *r*-Hepatocyte chimeric livers regain the normal arrangement of hepatic plates and sinusoids, reconstructing the resting liver structure with single hepatic plates along the portal-central axis at 5 weeks after transplantation (T-phase)
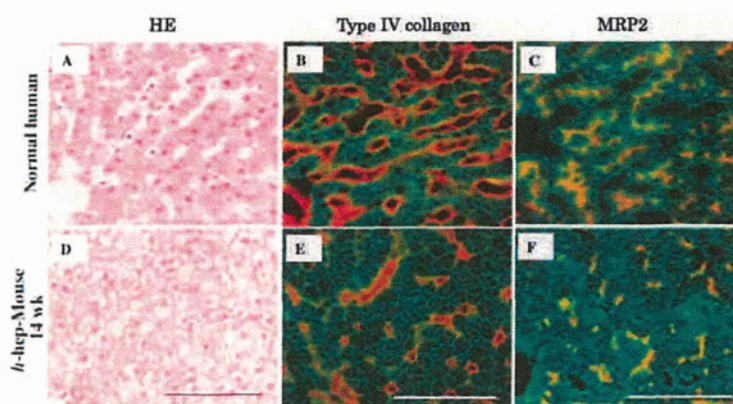
Fig. (6). Histological characteristics of *h*-hepatocyte chimeric mouse livers. Normal human livers were obtained from a 65-year-old female donor (**A-C**). *h*-Chimeric mice were generated by transplanting the hepatocytes from a 9-month-old male. The animals were sacrificed at 14 weeks (T-phase, **D–F**). Liver sections were stained with H&E (**A** and **D**) and for type IV collagen (red, **B** and **E**) and MRP2 (red, **C** and **F**). The sections of B, C, E, and F were additionally stained hCK8/18 (green) to identify transplanted *h*-hepatocytes. Scale bars shown in D, E, and F represent 100 μm. These Photos are cited from the literature No. 9.
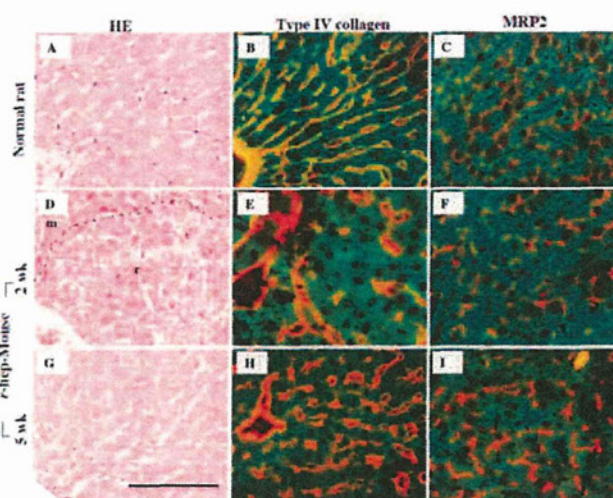

Fig. (7). Histological characteristics of *r*-hepatocyte chimeric mouse livers. Normal rat livers were obtained from 13-week-old male Fischer 344 rats (**A–C**). *r*-Hepatocyte chimeric mice were produced with 13-week-old male Fischer 344 rats and were sacrificed at two (P-phase, **D–F**) and five weeks (wks) after transplantation (T-phase, **G–I**). Liver sections were stained with H&E (**A, D, G**) and for type IV collagen (red, B, E, H) and MRP2 (red, **C, F, I**). The sections of B, C, E, F, H, and I were additionally stained for rRT1A (green) to identify transplanted *r*-hepatocytes. The dashed line in D shows the boundary between *r*-hepatocyte (r) and *m*-hepatocyte regions (m). Scale bar is shown in G and represents 100 μm. These Photos are cited from the literature No. 9.

(Fig. 7 G-I). Quite differently, *h*-hep chimeric livers do not show single-cell hepatic plates, but show multicell-layer-thick plates and have obscure structures of sinusoids, structures characteristic of proliferative liver, even though they are in T-phase (14 weeks post-transplantation) (Fig. **6 D-F**). The MRP2 protein is also still randomly distributed in the intercellular space. These histological features indicate that *r*-hepatocytes are able to repopulate the mouse liver, by rapidly proliferating therein, reconstructing liver structures, and terminating replication when the normal resting structures are regained with single-cell hepatic plates and distinct structures of sinusoids that are arranged in an orderly manner along the portal-central axis. In contrast, *h*-hepatocytes appear to continue to proliferate even after they reconstruct structurally complete livers and RIs arrive at a plateaus, which is in a good agreement with the above-mentioned observation that *h*-chimeric, but not *r*-chimeric, livers are much enlarged compared with the original *m*-livers. This liver swelling was not a result of *h*-hepatocytic hypertrophy, but *h*-hepatocytic hyperplasia, because our morphometric examinations about the length of the long axis of hepatocytes on H&E sections showed that there are no significant differences among *m*-, *r*- and *h*-hepatocytes in chimeric mice. Observation of the enlarged *h*-chimeric livers led us to assume that crosstalks between parenchyma and nonparenchyma cells concerning termination of hepatocyte proliferation in the liver are not adequate in *h*-chimeric liver.

HYPERPLASIS OF CHIMERIC MOUSE LIVER

Liver is quite powerful in the regenerative ability [16]. When damaged, it somehow recognizes the presence of damaged cells and starts to increase DNA synthesis quite
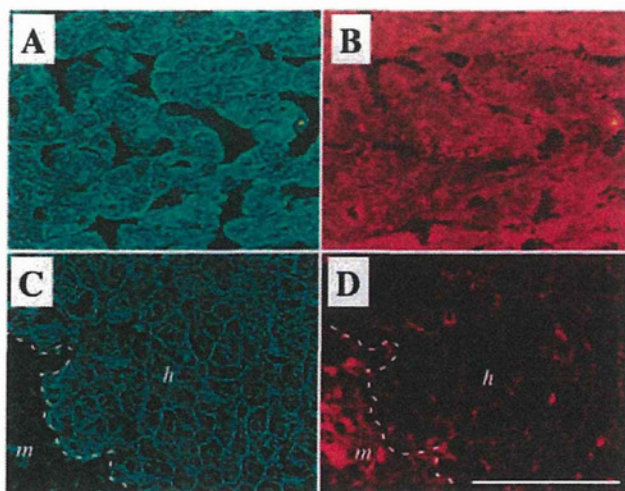
Fig. (8). Expression of TGFBR2 in normal and *h*-chimeric mouse livers. A 49-year-old male liver tissues were used as control normal human liver (**A**, **B**). uPA/SCID mice were transplanted with *h*-hepatocytes from 9-month-old male and sacrificed at 11 weeks (T-phase) after transplantation. The liver tissues were isolated from the mice (**C**, **D**). Liver sections were double stained for hCK8/18 for identifying *h*-hepatocytes (green; **A** and **C**) and TGFBR2 (red; **B** and **D**). The dashed lines in **C** and **D** indicate the boundary between *h*-hepatocyte (*h*) and *m*-hepatocyte regions (*m*). Scale bar represents 100 μm.

soon (within 24 h) for cell division to replace the damaged cells, but correctly terminates DNA synthesis/cell division when the mass ratio of the liver to the body weight reaches to a defined value determined by intercellular signaling between parenchymal and nonparenchymal cells [17], although underlying mechanisms have not been still completely understood. Studies with cultured hepatocytes suggested that TGF-β and its type II receptor TGFBR2 (TGF-β/TGFBR2) are antimitogenic for hepatocytes [18]. Two research groups independently generated hepatocyte-targeted TGFBR2-knockout mice and examined the role of TGF-β/TGFBR2 signaling in the termination of partial (70%) hepatectomy-induced liver regeneration, one by Romero-Gallo *et al.* claiming that TGF-β/TGFBR2 is a terminating factor [19] and the other by Oe *et al.* suggesting that activin A may be a principal terminator [20].

Based upon these previous studies, we asked whether TGF-β/TGFBR2 or activin A is involved in the observed hepatic hyperplasia in *h*-chimeric mouse [9]. The livers from *h*- and *r*-hepatocytes chimeric mice generated as above were examined for the expression levels of TGFBR1, TGFBR2, and Activin A type IIA receptor (ACVR2A) genes during repopulation of xenogeneic hepatocytes. The obtained expression levels were compared to those of the respective resting normal livers determined in the parallel experiments. Expressions of all these genes in *r*-hepatocyte chimeric mouse livers were suppressed to half those of normal rat livers in P-phase (at 2 weeks after transplantation, RI = 57%) and rapidly returned to normal levels in T-phase (at 3 weeks, RI = 97%) and were saturated thereafter (at 4 weeks, RI = 99%), suggesting roles of these genes as replication termination signals. In *h*-hepatocyte chimeric mouse livers, h-

TGFBR1 showed a similar expression pattern as rTGFBR1 in *r*-hepatocyte chimeric mouse livers except that changes progressed quite slowly taking 11 weeks after transplantation to regain normal levels. The expression levels of TGFBR2 and ACVR2A genes were also lower than the resting livers, the extent of suppression being quite prominent, less than one-third on the normal level. However, importantly *h*-hepatocyte chimeric livers kept the reduced levels thereafter up to 11 weeks after transplantation. The expression levels of TGFBR2 strictly down-regulated during the experimental period and those of ACVR2A showed a tendency to increase, but still much lower than the normal levels even at 11 weeks after transplantation.

We then immunohistologically tested our explanation of *h*-chimeric liver enlargement that *h*-hepatocytes fail to regain expression of TGFBR2 at a level seen in the normal resting liver in T-phase [9]. Liver sections at P- and T-phase from *h*- and *r*-hepatocyte chimeric livers were doubly stained with antibodies against "hCK8/18 and h/rTGFBR2 (cross-reactive for both humans and rats)" and "rRT1A (rat major histocompatibility complex class 1, for staining *r*-hepatocytes) and h/rTGFBR2", respectively, together with sections from normal resting human and rat livers. *r*-Hepatocytes in both normal rats and *r*-chimeric mice at T-phase were heavily positive to TGFBR2. Similarly *h*-hepatocytes in resting normal livers were heavily positive to TGBR2 (Fig. 8A and B), but not only those in P-phase at 5 weeks after transplantation, but also those in T-phase (11 weeks) were negative (Fig. 8C and D for *h*-hepatocytes in T-phase) as we thought. There were some positive cells, but these cells were identified as *m*-nonparenchyma cells by their morphology and distribution patterns. These results indicate that the hyperplasia caused by *h*-hepatocyte repopulation might be a result of persistent low sensitivity of *h*-hepatocytes in *h*-hepatocyte chimeric mouse toward TGF-β/activin, especially TGF-β. As mentioned above, TGFR1 mRNA was increased to the normal level at T-phase, which, however, appears not to affect the sensitivity of *h*-hepatocyte to the ligand, because TGF-β initially binds to TGFBR2 homodimers, which recruits TGFBR1 dimers forming a hetero-tetrameric complex, and TGF-β signals are transferred intracellularly [21].

The next question was which type of liver cells produce TGF-β as an anti-mitogenic factor for hepatocytes and induce them to get into T-phase when the host regains the correct $R_{L/B}$. TGF-β-expressing cells were identified by double immunostaining for desmin and TGF-β, which reveals the following facts: (1) When cells are positive for TGF-β, they are mostly desmin-positive; (2) Hepatic stellate cells of normal rats, normal humans, and SCID mice do not express TGF-β protein. Hepatic stellate cells are markedly activated and, as a result, increase their numbers and all express TGF-β protein at high levels in uPA/SCID mice (Fig. 9A, B); (3) In *r*-chimeric mice, the number of stellate cells markedly decreases and these cells do not express TGF-β protein in P-phase (Fig. 9C, D). Their number increases >4-fold as compared to P-phase and these cells all express TGF-β protein at considerably high levels in T-phase (Fig. 9G, H); (4) In *h*-chimeric mice, the number of stellate cells greatly decreases and these cells do not express TGF-β protein in P-phase as in *r*-chimeric mice (Fig. 9E, F). Their number increases >2-
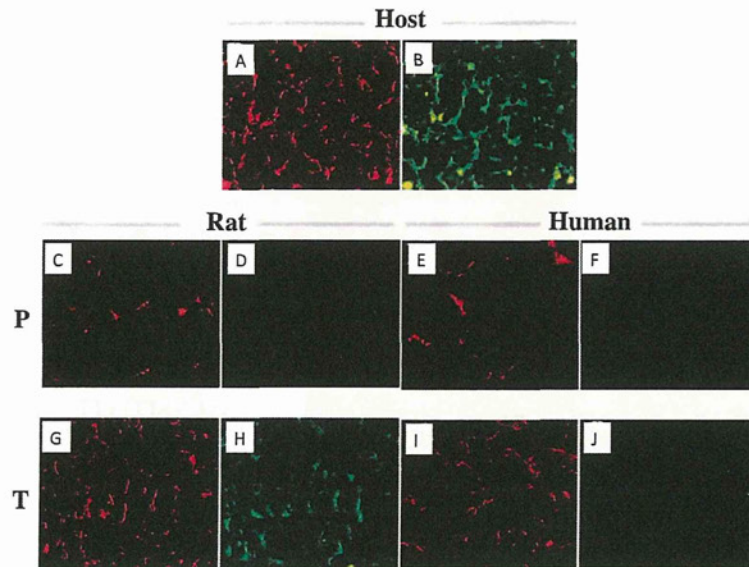
Fig. (9). Expression and distribution of TGF-β in normal and chimeric mouse livers. Livers were removed from a host mouse (1-month-old uPA/SCID mouse) (A, B), from *r*-chimeric mice with Fisher 344 rat hepatocytes (C, D, G, H) at P-phase (2 weeks post transplantation) (P: C, D) and at T-phase (three weeks post transplantation) (T: G, H) and from *h*-chimeric mice with 9-month-old male hepatocytes (E, F, I, J) at P-phase (five weeks post transplantation) (P: E, F) and at T-phase (11 weeks post transplantation) (T: I, J). These livers were cryosectioned and double-immunostained for desmin (A, C, G, E, I, red) and TGF-β (B, D, H, F, J, green). Serial sections from *r*- and *h*-hep-mouse livers were immunostained for rRT1A and hCK8/18 to identify *r*- and *h*-hepatocytes, respectively (data not shown). Scale bar represents 100 μm.
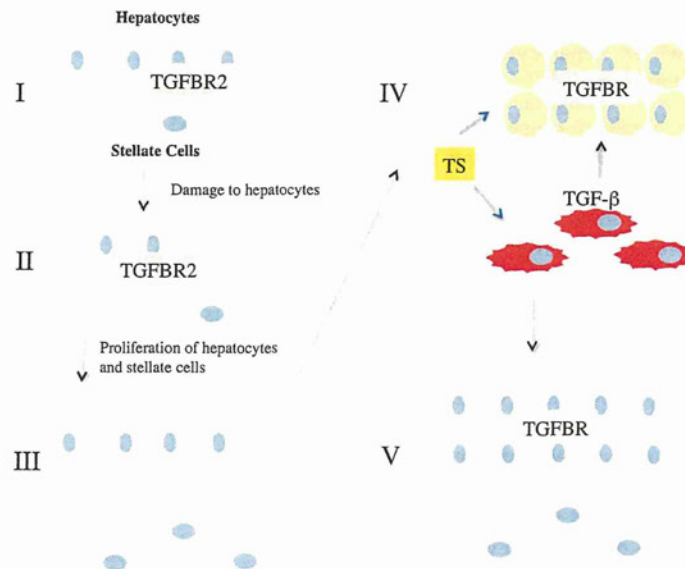

Fig. (10). Plausible interactions between hepatocytes and stellate cells to terminate the proliferation of hepatocytes during liver growth. Hepatocytes and stellate cells are in a normal resting state (Step I). Hepatocytes express TGFBR2. The liver is injured and the number of hepatocytes is reduced (Step II). The hepatocyts start to proliferate and get into Step III in which the TGFBR2 expression is reduced. When hepatocytes increase the number, which is adequate to sufficiently respond to metabolic demands of body. Such situations generate a termination signal(s) (TS), which makes hepatocyts to express TGFBR2 and activate stellate cells to express TGF-β (Step IV). The establishment of TGF-β signaling leads hepatocytes to terminate proliferation and stellate cells to terminate expression of TGF-β, which brings these cells into the resting state (Step V).

fold as compared to P-phase, but these cells all still do not express TGF-β protein in T-phase (Fig. **9I, J**), which is quite different from the case observed in *r*-chimeric mice.

These facts suggest that stellate cells are generally less distributed around proliferating hepatocytes in liver at P-phase and they do not produce TGF-β protein. However,
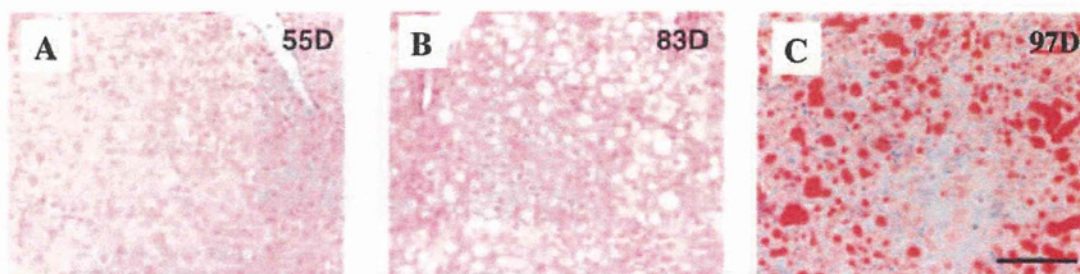
Fig. (11). Lipid accumulation in chimeric mouse *h*-hepatocytes. Chimeric mice with 6-year-old female were killed at 55 days (55D) (**A**) and 83 days (83 D) after transplantation for histological examinations of *h*-hepatocyte regions by H&E. No visible cytoplasmic vacuolation in the *h*-hepatocytes at 55 days, but extensive and intensive vacuolation at 83 days. *h*-Hepatocyte regions in the mice killed at 97 days (97D) were stained with Oil Red O together with nucler staining (blue). Bar represents100 μm. Photos are cited from the literature No. 10.

when the number of hepatocytes becomes close to the physiologically adequate number, stellate cells become abundantly distributed around the hepatocytes and these cells express TGF-β. These stellate cells cease to express TGF-β when the liver actually gets the adequate number of hepatocytes and become physiologically stable. *h*-Chimeric mouse liver are able to provide *h*-hepatocytes and *m*-stellate cells with environments which permit the progression to P-phase as in *r*-chimeric mouse liver, but these environments do not permit the progression to T-phase. The failure of TGF-β/TGFBR signaling in *h*-hepatocytes of *h*-chimeric mouse was supported by experiments in which we showed the absence of detectable levels of Smad2/3, major intracellular effectors in both TGFBR and ACVR, in *h*-hepatocyte nuclei in *h*-chimeric mouse livers at T-phase, contrasting to *r*-chimeric mouse livers whose hepatocyte nuclei contained high levels of the effector proteins [9].

The results we have obtained suggest the presence of plausible interactions between hepatocytes and stellate cells to terminate the proliferation of hepatocytes during liver growth (Fig. **10**). Hepatocytes in a normal resting state (Step I) express TGF-β type II receptor (TGFBR2). When the liver is injured (Step II), hepatocytes start to proliferate to recover the original number and get into Step III in which the TGFBR2 expression is reduced. When hepatocytes increase the number, which is adequate to normally respond to and treat metabolic demands of body (Step IV), the liver generates a termination signal(s) (TS), which makes hepatocytes to express TGFBR2 and activate stellate cells to express TGF-β. The establishment of TGF-β signaling leads hepatocytes to terminate proliferation and stellate cells to terminate expression of TGF-β, which brings these cells into the resting state (Step V). These hypothetical mechanisms could be applicable to interactions between *r*-hepatocytes and *m*-stellate cells due to phylogenetic closeness. Apparently, there are some failures in these mechanisms in the interactions between *h*-hepatocytes and *m*-stellate cells. One is that *m*-stellate cells are not able to proliferate or increase their number around *h*-hepatocytes (failure in Step III). Another is that hypothetical TS is not generated in Step IV and, thus, *h*-hepatocytes do not up-regulate TGFBR2 and *m*-stellate cells do not express TGF-β. Molecular entities of TS remain to be challenged for identifications.

INSENSITIVITY OF CHIMERIC MOUSE *H*-HEPATOCYTES TO MOUSE GH

Growth hormone (GH) is a key regulator of postnatal growth and metabolism [22] and exerts its effects by binding to its specific cell surface receptor, GH receptor (GHR), which triggers various intracellular signaling cascades [23]. GHR is a single transmembrane protein of class 1 cytokine receptor family [23, 24]. Exceptionally among peptide and protein hormones in mammals, although primate GH is effective to not only primates, but also to other mammals, non-primate mammalian GH is effective among non-primate mammals, but not to primates, which is called "species specificity" of GHR [25]. Arg^{43} in hGHR is responsible for the species specificity as GH/GHR binding, because replacement of Arg^{43} to Leu as in non-primate bovine GHR, for example bovine, greatly reduced its affinity to hGH [25].

Supporting the notion of GHR-species specificity, *h*-hepatocytes in *h*-chimeric mouse does not respond to mGH, because hIGF-1, the principal GH mediator [26], was undetectable even *h*-chimeric mice with RI >90%, which became detectable when the mice were treated with recombinant hGH [27]. GH was reported to stimulate liver regeneration induced by partial hepatectomy [28], which is especially noteworthy in relation to ageing. Hepatic regenerative capacity is generally decreased with ageing [29], which is associated with a progressive decline in GH secretion [30]. It was experimentally demonstrated that GH stimulated proliferation of old-aged regenerating liver through forkhead box m1b [31]. Involvement of GH in liver regeneration as a physiological pro-regeneration agent was also shown utilizing GH antagonist transgenic mice, in which the action of GH is blocked [32].

From these our and other researchers' studies we thought that *h*-chimeric mice are quite useful as an *in vivo* model to study effects of GH on human liver, because first the *h*-hepatocytes in the mice are in the hGH-deficient state and second GH shows physiological and pathological actions on liver including regeneration in an age-dependent manner. Meantime, we noticed the deposition of lipid droplets in *h*-hepatocytes of chimeric mice when the animals are reared for a relatively longer period of time (> ~70 days after transplantation). It is generally known that GH plays a major role in the regulation of lipid metabolism, and impairment in the GH axis elicits major changes in glucose and lipid metabolism [33].
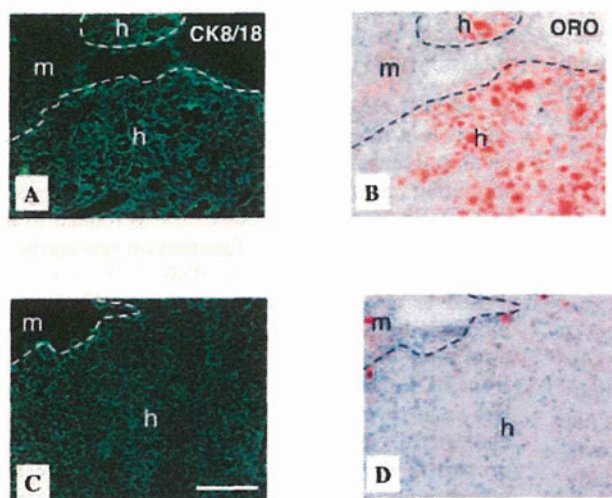
Fig. (12). Effects of hGH on liver steatosis. Two groups of chimeric mice with a 6-year-old girl's hepatocytes were used to test the effect of hGH on liver steatosis, one without treatment with hGH (A, B) and the other with the hormone treatment (C, D). The animals of the experimental group were given hGH in the last 2 wk before being killed 70–90 days after transplantation. Liver tissues were stained for hCK8/18 immunohistochemistry to identify *h*-hepatocytes (A, C). Primary antibodies were visualized with Alexa 594-conjugated anti-mouse IgG goat sera. Their serial sections were stained with Oil Red (ORD) (B, D). Small to large droplets are diffusely distributed in *h*-hepatocytes from control chimeric livers, but are absent in hGH-treated animals. m and h indicate regions of *m*- and *h*-hepatocytes, respectively. Dotted lines show the boundary between the two regions. Scale bar is shown in C and represents 100 μm. Photos are cited from the literature No. 10.

With these backgrounds we investigated hepatic lipogenesis in chimeric mouse liver in relation to GH-deficiency [10]. *h*-Chimeric mice transplanted with 6-year-old girl started to present vacuoles in the cytoplasm of donor hepatocytes around 70 days post-transplantation, which gradually increased in numbers and size thereafter (Fig. **11A** and **B**). These vacuoles were stainable with Oil Red O (ORO) (Fig. **11C**), thus, concluded to be lipid deposits. More than 90% of the tested chimeric mice whose RIs were >70% spontaneously became fatty 90 days post-transplantation. It was most plausible that the observed hepatic steatosis is induced by the lack of available hGH in the hosts and this possibility was soon verified by the following studies. Chimeric mice with RI >70% (hepatocytes from a 6-year-old girl) were infused with hGH at 2.5 mg/kg/day for the last 2 weeks of the transplantation experiments. As expected, GH administration raised the hIGF-1 serum concentration from undetectable levels to levels (~73 ng/ml) comparable to normal human serum levels and prominently abolished lipid granules (Fig. **12**). Thus, we conclude that first *h*-hepatocytes in *h*-chimeric mice are deprived of hGH, gradually accumulate lipid droplets, and finally become steatotic, and second hGH plays a principal role in the etiology of human liver steatosis [10].

Comparison of gene expression profiles between *h*-hepatocytes from hGH-untreated and -treated mice by microarray and real-time quantitative RT-PCR enabled us to identify the following 14 GH-up-regulated genes in the de-

scending sequence from the highest ratio to the lowest, ASCL1 (achaete-scute complex-like 1), IGF-I, SOCS2 (suppressor of cytokine signaling 2), nicotinamide N-methyltransfease, KL (klotho), P4AH1 (procollagen-proline, 2-oxoglutarate 4-dioxygenase, a-polypeptide 1), DSCR1L1 (down syndrome critical region gene 1-like1), IGFLS (IGF-binding protein, acid labile subunit), CREM (camp-responsive element modulator), MBL2 (mannose-binding lectin 2, soluble), AMIGO2 (adhesion molecule with Ig-like domain 2), C50RF13 (chromosome 5 open reading frame 13), SLC16A1 (solute carrier family 16, member 1), and SRD5A1 (steroid-5-a-reductase, a-polypeptide 1), together with 4 GH-down-regulated genes such as FADS1 (fatty acid desaturase 1), PCOLCE22 (procollagen C-endopeptidase enhancer 2), AKR1B10 (aldo-keto reductase family 1, member B10), and SERPINE1 (serine proteinase inhibitor, clade E, member 1). Actually, when the expression levels of these genes were compared to those in normal human livers, most of the former and latter genes were down- and up-regulated in *h*-chimeric mouse livers, respectively, except that KL was not down-regulated in chimeric mice [10].

Among them, ASCL1, or also termed ASH1 (achaete-scute homolog 1), is a basic helix-loop-helix transcription factor, and might be worthy to be considered in relation to hepatic steatosis observed in *h*-chimeric mice, because Hes6 is included as the target genes of ASCL1 [34]. Recently, Talianidis and coworkes identified Hes6 as a novel HNF4a target and reported that these two transcription factors regulate the gene expressions responsible for hepatic fatty acid metabolism such as CPT1, Acot1, FGF21, HMGCS2, and CD36, coordinating with PPARα and γ [35].

There are studies that show reciprocal regulations of GH and SOCS-2 expressions. GH increases the expression of SOCS-2 in cultured rat hepatocytes [36] and in mouse liver *in vivo* [37], which supports our results. In contrast, SOCS-2 appears to negatively regulate the expression of GH, because deletion of SCCS-2 genes results in increase of GH signaling including lipogenesis [38, 39]. STAT5β is a transcription factor that associates with intracellular domain of the GHR. Upon GH stimulation, STAT5β is phosphorylated by Janus kinase (JAK), dimerizes, translocated to nucleus, and promotes the transcription of some GH-regulated genes [40]. SOCS2 is one of the STAT5β target genes and its promoter regions contain an E-box followed by STA5β binding sites, both of which are shown to be required for full GH responsiveness [40]. Activities of intracellular GH signaling through Stat5a and Stat5b seem to be high in GH-treated *h*-chimeric mouse hepatocytes, which might induce SOCS-2 gene expression and its gene products might contribute to homeostasis of GH signaling and lipid metabolism.

Regarding the upregulation of P4HA1 in h-GH treated *h*-hepatocytes, it is relevant to state three points: firstly proly 4-hydroxylase (P4H), a α2β2 heterodimer, plays a critical role(s) in biosynthesis and formation of all known types of collagen, the representative extracellular matrix necessary for growth and morphology of tissues, and the abundance of the α–subunit restricts the enzymatic activity [41]; second, its gene transcription is mediated through binding of upstream stimulatory factors with its E-box-containing pro-

moter regions [41], suggesting GH-signaling pathway could be involved in this regulation as in SOCS-2; third, however, biological significance of up-regulation of P4HA1 gene by h-GH remains unclear, because it is generally known that hepatocytes do not express collagen genes in both biological and pathological conditions [42]. The upregulation of P4Ha1 gene by hGH appears not to be related with lipolysis observed in hGH-treated chimeric livers.

At least two possibilities are considered for the role of DSCR1-L1 (or termed rcan2), which is known to inhibit calcineurin signaling. It was reported that cyclosporine A, an inhibitor of calcineulin, inhibits apolipoprotein A1 (apAI) gene expression [43]. Thus, DSCR1-L1 plays a role in regulating amounts of lipid through balancing high density lipoprotein (HDL) metabolism. Or this gene expression does not reflect the lipid metabolism, but reflect hyperplastic growth of *h*-hepatocytes in *h*-chimeric mouse, because a study showed that bax inhibitor-1 (BI-1) regulates liver regeneration through dephosphorylation and nuclear translocation of nuclear factor of activated T cells (NFATI) by calcineurin [44]. CREM is a transcription factor that binds to the cAMP response element (CRE) found in a number of gene promoters. To our knowledge, there have no reports whether lipid metabolism-associated genes are included in the target genes of CREM. Interestingly, CREM gene was reported as hGH-upregulated genes in which gene expression in peripheral blood mononuclear cells was compared between children with GH deficient (GHD) and those hGH-treated children with GHD [45].

Significance of upregulation of MBL2, a protein of the humoral innate immune system, is not clear in relation to GH signaling and lipid metabolism. However, MBL2 might play a role in activating lipid metabolisms, because MBL2 gene expression was reported to be significantly up regulated in *h*-hepatocytes by Wy14643, an agonist of peroxisome proliferator-activated receptor alpha (PPARα) which is known to be activated by endogenous agonists such as fatty acids and fatty acid derivatives [46]. C5ORF13 gene, also known as P113 gene, is a gene originally discovered as abundant transcript at site of active embryonic and postnatal nerurogenesis [47]. Recently, the possibility was proposed that C5ORF13 upregulates several classes of genes associated with lipid synthesis in a retinoic acid dependent manner [48]. It is plausible that the retinoic acid/C5ORF13 signaling functions in choresterol and lipid homeostasis in hGH-treated chimeric mouse hepatocytes.

SRD5A1 converts testosterone into 5-alpha-dihydrotestosterone, a potent androgen hormone, and progesterone or corticosterone into their corresponding 5-alpha-3-oxosteroids. This enzyme could be involved in hGH-dependent lipid metabolism, because it was reported that first GH up-regulated SRD5A1 and GHR in cultured haematopoietic cells [49], and second, a study with mice lacking hepatic androgen receptor (AR) suggested that AR may play a vital role in preventing the development of hepatic steatosis [50]. We currently consider that hGH-induced upregulation of SL16A1 gene is not related to lipid metabolism, but to hyperplastic growth of *h*-hepatocytes in *h*-chimeric liver,

because it was reported that miR-124 whose target gene was identified as SL16A1 gene is down-regulated in medulloblastoma [51].

FADS1 encodes the membrane bound delta-6 desaturase, which is a rate-limiting enzyme for the formation of long-chain polyunsaturated fatty acids and plays a key role in determining plasma and tissue fatty acid profiles [52]. PCOLCE2, now known as PCPE2, is related to the lipid metabolism by its regulatory function on pro-apolipoprotein A-I (pro-apoA-I) processing by BMP-1 to apoA-1 that is exported to circulation and associated with HDL [53]. HDL binds cholesterols produced from peripheral tissue cells and transports them to hepatocytes, which remove cholesteros from HDL particles and eliminate them into bile, the process known as reverse cholesterol transport (RCT) responsible for cholesterol clearance [54]. ApoA-I is the principal protein present in the outer hydrophilic phase of the HDL particle whose inner hydrophobic phase contains phospholipids and cholesterol esters, and its structure modulates HDL function [55]. It is thought that in pro-apoAI and BMP-1 or BMP-1 and PCOLCE1/PCPE2 first are associated and then a ternary complex of pro-apoAI/BMP-1/PCPE2 is formed in the cytoplasm, in which PCPE2 might play a chaperon-like function or enhance BMP-1's processing of pro-apoAI [53]. Based upon a series of experiments to investigate the mechanism of interactions among PCPE2, apoA-I, and BMP2, Zhu et al. (2009) have proposed that although currently the functional significance of the apoA-1 processing is unclear, its prosegment might as an activator or repressor of the processing of apoA-I depending its concentration [53], by which we speculate, PCPE2 levels could regulate HDL-C–dependent lipid metabolisms.

AKR1B10, also designated aldose reuctase-like-1 (ARL-1), is known to participate in the pathway of lipid synthesis through stabilizing acetyl-CoA carboxylase as an rate-limiting enzyme of *de nove* synthesis of long chain fatty acids [56]. Serpine1, commonly called plasminogen activator inhibitor-1 (PAI-1), might be related to hepatic lipid metabolism, because hepatocytes are reported as PAI-secreting cells [57]. Its plasma levels are elevated in nonalcoholic steatohepatitis (NASH) patients [58]. The promoter region of its gene shows several response elements related with either metabolic or inflammatory pathways including very-low-density lipoprotein [59], and its gene is dramatically upregulated in steatohepatitis [60]. There is also a study that showed the correlation of liver fat content with serum level of serpine1 [61].

RESPONSES OF CHIMERIC MOUSE LIVER TO HUMAN HEPATITIS VIRUSES

Chimpanzees had been used for efficacy studies of antiviral drugs as HBV- and HCV-susceptible animals [62]. However, chimpanzees have been becoming less accessible for experimental uses because of expensiveness and animal welfare regulations. Since the advent of *h*-hepatocyte chimeric mouse [3, 4], researchers have recognized its usefulness as an appropriate animal model for study on HBV and HCV. Although studies on HBV/HCV using chimeric mice are still progressively increasing worldwide, in this review we just summarize major studies performed in our group or

in association with our group. These mice are susceptible to HBV and HCV and maintain viremia with high titers for long term [5]. They were successfully infected with HBV-containing serum or genetically engineered HBV, and their viremia levels were effectively reduced by administration of Lamivudin, which indicates that the chimeric mouse model is also usable for R&D of anti-HCV/HBV drugs [5]. Lamivudine-resistant mutated HBV were insensitive to Lamivudin compared to non-mutated HBV [63]. It has been assumed that the non-structural X protein of HBV, HBx, plays an important role in HBV replication, which was supported by a study using the chimeric mice demonstrating that HBx protein is indispensable for development of viremia in the chimeric mice [64]. A study with chimeric mice also contributed to elucidating poorly understood cytopathic effects of HBV and its association with particular viral genotypes or genetic mutations, which demonstrated that different HBV genotypes resulted in different virologic and histopathologic outcome of infection, and particular genetic variants of HBV may be directly cytopathic in immunosuppressive conditions [65].

There have been studies showing efficacy of candidates of anti-HCV drugs using HCV-infected chimeric mice: Myriocin (Serine palmitoyltransferase inhibitor) [66], 17-(dimethylaminoethylamino)-17-demethoxygeldanamycin (HSP90 inhibitor) [67], DEBIO-025 (cyclophilin Inhibitor) [68], NS3-4A and NS5B protease inhibitor [69, 70], and an inhibitor of 24-dehydrocholesterol reductase (DHCR24) [71]. These accumulating data all show that the chimeric mouse model of HBV or HCV infection is a quite useful tool for the study of HBV or HCV virology and evaluation of anti-viral drugs.

RESPONSES OF CHIMERIC MOUSE LIVER TO DRUGS

Compared to studies on HCV/HBV, chimeric mice have been less utilized for studies to predict human metabolisms of drugs, but their usefulness has been increasingly appreciated among researchers in pharmaceutical areas [7, 8]. In this review we briefly introduce recent progresses of studies of drug metabolisms using chimeric mice. It is generally known that cytochrome P450 enzymes (CYPs) play an important role in the metabolism of medicines and other xenobiotics [7, 8]. The presence of animal species differences in the metabolism of many drugs is the key factor in adopting chimeric mouse model for R&D of medical drugs. In the chimeric mouse liver, expressions of human enzymes that play critical roles in drug metabolisms have been reported including cytochrome P450 enzymes such as CYPs, CYP1A1, 1A2, 2A6, 3A4, 3A5, 2C9, 2C8, 2C19, and 2D6), phase II enzymes (UGT, SULT, CST, TPST, NAT, PEMT, and AMST), and also aldehyde oxigenase [6, 72-77]. Recently, it was reported that S-warfarin is metabolized to S-7-hydroxywarfarin, catalyzed by CYP2C9, and is primarily recovered in urine in humans [78]. Mass balance and metabolic disposition of S-warfarin in chimeric mice is similar to the reported human data [79, 80]. These currently available data, although still not so abundant, strongly suggest that chimeric mice are a useful and powerful model for the examination of absorption, distribution, metabolism, and excretion (ADME) and

drug interactions via enzyme induction and inhibition *In vivo* [6-8, 74-79].

Regarding utilization of chimeric mouse in drug development, it is relevant here to refer to *h*-hepatocytes isolated from chimeric mouse livers. Cryopreserved *h*-hepatocytes are currently regarded as the best *in vitro* model for predicting human intrinsic clearance of xenobiotics in spite of the fact that fresh *h*-hepatocytes have greater plating efficiency on dishes and greater metabolic activities than cryopreserved cells, because experimentation for reproducible studies using fresh hepatocytes from the same donor is not practical and an "on demand" supply of fresh hepatocytes is not realistic. Recently, we sought for the possibility that the chimeric mouse could serve as a novel source of fresh *h*-hepatocytes for *in vitro* studies [81]. *h*-Hepatocytes were isolated from chimeric mice, and CYP activities were determined. Expressions of CYP1A2, 2C9, 2C19, 2D6, 2E1, 3A and glucuronidation of fresh hepatocytes derived from chimeric mice were equal or superior to cryopreserved cells. Thus, we propose that chimeric mice could be precious sources of fresh *h*-hepatocytes on demand that retain high and stable phase I enzymes and glucuronidation activities.

PERSPECTIVES

In the previous reviews we described a short research history on the advent of a *h*-chimeric mouse and its utilization as a convenient animal model that is small-sized, relatively easy in maintaining in laboratory, and easy in experimental handlings for drug testing and HBV/HCV-infection studies [7, 8]. As stated therein and in the present review, *h*-chimeric mice have been increasingly utilized among researchers as such models, because hitherto accumulated experiences with *h*-chimeric mice have showed that the liver tissues composed of human parenchymal cells and mouse nonparenchymal cells in mouse body appreciably represent the phenotypes of liver tissues of human body, although not perfectly, and are practically quite useful if we utilize the model recognizing its limitations.

One of the major limitations inherent to the current *h*-chimeric mouse model is the incomplete replacement of *m*-hepatocytes with *h*-hepatocytes. Although it is possible to generate chimeric mice with RI = ~100% ("complete" *h*-chimeric mouse) under appropriate conditions with adequate animal cares for the sake of a purely research purpose, chimeric mice with RI = 70 - 80% are practical for industrial drug R&D activities and sufficient for usual studies for HBV/HCV infection mechanisms. However, a problematic case was reported in which chimeric mice had been administered with a test drug that is well metabolized by *m*-hepatocytes, but to a limited extent by *h*-hepatocytes and its mouse metabolites include all its human metabolites [82]. In this case the serum metabolic profile was closely similar to that of the control mice, and no significant increase in the peaks of human metabolites were found. To avoid this type of problems coming from metabolic activities by the residual *m*-hepatocytes, we have to develop a technology by the residual host hepatocytes can be specifically eliminated from the currently available chimeric mice with with RI = 70 - 80%.

Unlike previous reviews, we emphasize herein the dissimilarity in biological features between artificial *h*-hepatocyte chimeric livers and natural human livers based upon the facts obtained in our recent studies that chimeric livers are under hyperplasia and under GH-deficiency, hoping to provide researches with our current opinions on *h*-chimeric mouse model. First, it should be noted that in spite of the presence of these dissimilarities *h*-chimeric mice have been shown to be practically quite useful at least for pharmaceutical researches and virological studies on HCB/HBV if researchers correctly understand merits and demerits in utilizing the animals in relation to the aims of their studies. Secondly, it is apparent that knowing the presence of dissimilarity will give us ideas and hints to generate a *h*-chimeric mouse whose liver shows biological features much closer to natural human livers than currently available *h*-chimeric mice. For example, livers of *h*-chimeric mice given appropriate amounts of hGH depending on the purposes of researches could reproduce the situations more resembling human livers and, thus, such a modified chimeric mouse will be an appropriate model for studying age-dependent changes in drug metabolisms and virological infections.

Although not referred to in this review, lack of human systems of inflammations and immunological recognitions in the current chimeric mice largely limit the usability of the *h*-chimeric mouse model in the study of pathological processes induced by drugs and viruses. Introduction of these systems into the *h*-chimeric mice will be a big and attractive challenge to generate a more useful humanized mouse liver model.

CONFLICT OF INTEREST

Declared none.

REFERENCES

[1] Nakanishi Y, Matsushita A, Matsuno K, *et al*. Regional distribution of drug-metabolizing enzyme activities in the liver and small intestine of cynomolgus monkey. Drug Metab Pharmacokinet 2011; 26(3): 288-94.

[2] Wilkinson GR. Drug metabolism and variability among patients in drug response. N Engl J Med 2005; 352: 2211-21.

[3] Mercer DF, Schiller DE, Elliott J, *et al*. Hepatitis C virus replication in mice with chimeric human livers. Nat Med 2001; 7: 927-33.

[4] Dandri M, Burda MR, Török E, *et al*. Repopulation of mouse liver with human hepatocytes and *In vivo* infection with hepatitis B virus. Hepatology 2001; 33: 981-8.

[5] Tsuge M, Hiraga N, Takaishi H, *et al*. Infection of human hepatocyte chimeric mouse with genetically engineered hepatitis B virus. Hepatology 2005; 42: 1046-54.

[6] Tateno C, Yoshizane Y, Saito N, *et al*. Near completely humanized liver in mice shows human-type metabolic responses to drugs. Am J Pathol 2004; 165: 901-12.

[7] Yoshizato K, Tateno C. A human hepatocyte-bearing mouse: an animal model to predict drug metabolism and effectiveness in humans. PPAR Res 2009; 2009: 476217.

[8] Yoshizato K, Tateno C. *In vivo* modeling of human liver for pharmacological study using humanized mouse. Expert Opin Drug Metab Toxicol 2009; 5: 1435-46.

[9] Utoh R, Tateno C, Kataoka M, *et al*. Hepatic hyperplasia associated with discordant xenogeneic parenchymal-nonparenchymal interactions in human hepatocyte-repopulated mice. Am J Pathol 2010;

[10] Tateno C, Kataoka M, Utoh R, *et al*. Growth hormone-dependent pathogenesis of human hepatic steatosis in a novel mouse model bearing a human hepatocyte-repopulated liver. Endocrinology 2011; 152: 1479-91.

[11] Baratta JL, Ngo A, Lopez B, Kasabwalla N, Longmuir KJ, Robertson RT. Cellular organization of normal mouse liver: a histological, quantitative immunocytochemical, and fine structural analysis. Histochem Cell Biol 2009; 131: 713-26.

[12] Wake K. Functional heterogeneity of liver tissue: from cell lineage diversity to sublobular compartment. In sinusoidal structure and dynamics (Ed. Vidal-Vanaclocha F). Springer and R.G.Landes Company 1997, 57-67.

[13] Rhim JA, Sandgren EP, Palmiter RD, Brinster RL. Complete reconstitution of mouse liver with xenogeneic hepatocytes. Proc Natl Acad Sci USA 1995; 92: 4942-6.

[14] Wack KE, Ross MA, Zegarra V, Sysko LR, Watkins SC, Stolz DB. Sinusoidal ultrastructure evaluated during the revascularization of regenerating rat liver. Hepatology 2001; 33: 363-78.

[15] Martinez-Hernandez A, Delgado FM, Amenta PS. The extracellular matrix in hepatic regeneration. Localization of collagen types I, III, IV, laminin, and fibronectin. Lab Invest 1991; 64: 157-66.

[16] Koniaris LG, McKillop IH, Schwartz SI, Zimmers TA. Liver regeneration. J Am Coll Surg 2003; 197: 634-59.

[17] Yoshizato K, Tateno C, Utoh R. The Mechanism of liver size control in mammals: a novel animal study. Int J Des Nat Ecodyn 2009; 4: 123-42.

[18] Russell WE. Transforming growth factor beta (TGF-beta) inhibits hepatocyte DNA synthesis independently of EGF binding and EGF receptor autophosphorylation. J Cell Physiol 1988; 135: 253-61.

[19] Romero-Gallo J, Sozmen EG, Chytil A, *et al*. Inactivation of TGF-beta signaling in hepatocytes results in an increased proliferative response after partial hepatectomy. Oncogene 2005; 24: 3028-41.

[20] Oe S, Lemmer ER, Conner EA, *et al*. Intact signaling by transforming growth factor beta is not required for termination of liver regeneration in mice. Hepatology 2004; 40: 1098-105.

[21] Ten Dijke P, Miyazono K, Heldin CH. Signaling via hetero-oligomeric complexes of type I and type II serine/threonine kinase receptors. Curr Opin Cell Biol 1996; 8: 139-45.

[22] Veldhuis JD, Roemmich JN, Richmond EJ, *et al*. Endocrine control of body composition in infancy, childhood, and puberty. Endocr Rev 2005; 26: 114-46.

[23] Piwien-Pilipuk G, Huo JS, Schwartz J. Growth hormone signal transduction. J Pediatr Endocrinol Metab 2002; 15: 771-86.

[24] Wei Y, Rhani Z, Goodyer CG. Characterization of growth hormone receptor messenger ribonucleic acid variants in human adipocytes. J Clin Endocrinol Metab 2006; 91: 1901-8.

[25] Souza SC, Frick GP, Wang X, Kopchick JJ, Lobo RB, Goodman HM. A single arginine residue determines species specificity of the human growth hormone receptor. Proc Natl Acad Sci USA 1995; 14; 92: 959-63.

[26] Castellano G, Affuso F, Conza PD, Fazio S. The GH/IGF-1 Axis and Heart Failure. Curr Cardiol Rev 2009; 5: 203-15.

[27] Masumoto N, Tateno C, Tachibana A, *et al*. GH enhances proliferation of human hepatocytes grafted into immunodeficient mice with damaged liver. J Endocrinol 2007; 194: 529-37.

[28] Asakawa K, Hizuka N, Takano K, *et al*. Human growth hormone stimulates liver regeneration in rats. J Endocrinol Invest 1989; 12: 343-7.

[29] Bucher NL, Swaffield MN, Ditroia JF. The influence of age upon the incorporation of thymidien-2-C14 into the DNA of regenerating rat liver. Cancer Res 1964; 24: 509-12.

[30] Rudman D, Feller AG, Nagraj HS, *et al*. Effects of human growth hormone in men over 60 years old. N Engl J Med 1990; 323: 1-6.

[31] Krupczak-Hollis K, Wang X, Dennewitz MB, Costa RH. Growth hormone stimulates proliferation of old-aged regenerating liver through forkhead box m1b. Hepatology 2003; 38: 1552-62.

[32] Pennisi PA, Kopchick JJ, Thorgeirsson S, LeRoith D, Yakar S. Role of growth hormone (GH) in liver regeneration. Endocrinology 2004; 145: 4748-55.

[33] Sangiao-Alvarellos S, Vázquez MJ, Varela L, *et al*. Central ghrelin regulates peripheral lipid metabolism in a growth hormone-independent fashion. Endocrinology 2009; 150: 4562-74.

[34] Hu Y, Wang T, Stormo GD, Gordon JI. RNA interference of achaete-scute homolog 1 in mouse prostate neuroendocrine cells

177: 654-65.

reveals its gene targets and DNA binding sites. Proc Natl Acad Sci USA 2004; 101: 5559-64.

[35] Martinez-Jimenez CP, Kyrmizi I, Cardot P, Gonzalez FJ, Talianidis I. Hepatocyte nuclear factor 4alpha coordinates a transcription factor network regulating hepatic fatty acid metabolism. Mol Cell Biol 2010; 30: 565-77.

[36] Tollet-Egnell P, Flores-Morales A, Stavréus-Evers A, Sahlin L, Norstedt G. Growth hormone regulation of SOCS-2, SOCS-3, and CIS messenger ribonucleic acid expression in the rat. Endocrinology 1999; 140: 3693-704.

[37] Adams TE, Hansen JA, Starr R, Nicola NA, Hilton DJ, Billestrup N. Growth hormone preferentially induces the rapid, transient expression of SOCS-3, a novel inhibitor of cytokine receptor signaling. J Biol Chem 1998; 273: 1285-7.

[38] Cui Y, Hosui A, Sun R, et al. Loss of signal transducer and activator of transcription 5 leads to hepatosteatosis and impaired liver regeneration. Hepatology 2007; 46: 504-13.

[39] Rico-Bautista E, Greenhalgh CJ, Tollet-Egnell P, et al. Suppressor of cytokine signaling-2 deficiency induces molecular and metabolic changes that partially overlap with growth hormone-dependent effects. Mol Endocrinol 2005; 19: 781-93.

[40] Vidal OM, Merino R, Rico-Bautista E, et al. In vivo transcript profiling and phylogenetic analysis identifies suppressor of cytokine signaling 2 as a direct signal transducer and activator of transcription 5b target in liver. Mol Endocrinol 2007; 21: 293-311.

[41] Chen L, Shen YH, Wang X, et al. Human prolyl-4-hydroxylase alpha(I) transcription is mediated by upstream stimulatory factors. J Biol Chem 2006; 281: 10849-55.

[42] Lasher CD, Rajagopalan P, Murali TM. Discovering networks of perturbed biological processes in hepatocyte cultures. PLoS One 2011; 6: 15247.

[43] Zheng XL, Wong NC. Cyclosporin A inhibits apolipoprotein AI gene expression. J Mol Endocrinol 2006; 37: 367-73.

[44] Bailly-Maitre B, Bard-Chapeau E, Luciano F, et al. Mice lacking bi-1 gene show accelerated liver regeneration. Cancer Res 2007; 67: 1442-50.

[45] Whatmore AJ, Patel L, Clayton PE. A pilot study to evaluate gene expression profiles in peripheral blood mononuclear cells (PBMCs) from children with GH deficiency and Turner syndrome in response to GH treatment. Clin Endocrinol (Oxf) 2009; 70: 429-34.

[46] Rakhshandehroo M, Hooiveld G, Müller M, Kersten S. Comparative analysis of gene regulation by the transcription factor PPARalpha between mouse and human. PLoS One 2009; 4: 6796.

[47] Studler JM, Glowinski J, Lévi-Strauss M. An abundant mRNA of the embryonic brain persists at a high level in cerebellum, hippocampus and olfactory bulb during adulthood. Eur J Neurosci 1993; 5: 614-23.

[48] Leung JK, Cases S, Vu TH. P311 functions in an alternative pathway of lipid accumulation that is induced by retinoic acid. J Cell Sci 2008; 121: 2751-8.

[49] Paparini A, Impagnatiello F, Pistilli A, et al. Identification of candidate genes and expression profiles, as doping biomarkers. Ann Ig 2007; 19: 303-14.

[50] Lin HY, Yu IC, Wang RS, et al. Increased hepatic steatosis and insulin resistance in mice lacking hepatic androgen receptor. Hepatology 2008; 47: 1924-35.

[51] Li KK, Pang JC, Ching AK, et al. miR-124 is frequently downregulated in medulloblastoma and is a negative regulator of SLC16A1. Hum Pathol 2009; 40: 1234-43.

[52] Merino DM, Ma DW, Mutch DM. Genetic variation in lipid desaturases and its impact on the development of human disease. Lipids Health Dis 2010; 18; 9: 63.

[53] Zhu J, Gardner J, Pullinger CR, Kane JP, Thompson JF, Francone OL. Regulation of apoAI processing by procollagen C-proteinase enhancer-2 and bone morphogenetic protein-1. J Lipid Res 2009; 50: 1330-9.

[54] Camarota LM, Chapman JM, Hui DY, Howles PN. Carboxyl ester lipase cofractionates with scavenger receptor BI in hepatocyte lipid rafts and enhances selective uptake and hydrolysis of cholesteryl esters from HDL3. J Biol Chem 2004; 279: 27599-606.

[55] Huang R, Silva RA, Jerome WG, et al. Apolipoprotein A-I structural organization in high-density lipoproteins isolated from human plasma. Nat Struct Mol Biol 2011; 8: 416-22.

[56] Wang C, Yan R, Luo D, Watabe K, Liao DF, Cao D. Aldo-keto reductase family 1 member B10 promotes cell survival by regulat-

ing lipid synthesis and eliminating carbonyls. J Biol Chem 2009; 284: 26742-8.

[57] Anfosso F, Chomiki N, Alessi MC, Vague P, Juhan-Vague I. Plasminogen activator inhibitor-1 synthesis in the human hepatoma cell line Hep G2. Metformin inhibits the stimulating effect of insulin. J Clin Invest 1993; 91: 2185-93.

[58] Targher G, Bertolini L, Scala L, et al. Plasma PAI-1 levels are increased in patients with nonalcoholic steatohepatitis. Diabetes Care 2007; 30: 31-2.

[59] De Taeye B, Smith LH, Vaughan DE. Plasminogen activator inhibitor-1: a common denominator in obesity, diabetes and cardiovascular disease. Curr Opin Pharmacol 2005; 5: 149-54.

[60] Matsuzawa N, Takamura T, Kurita S, et al. Lipid-induced oxidative stress causes steatohepatitis in mice fed an atherogenic diet. Hepatology 2007; 46: 1392-403.

[61] Ishii M, Yoshioka Y, Ishida W, et al. Liver fat content measured by magnetic resonance spectroscopy at 3.0 tesla independently correlates with plasminogen activator inhibitor-1 and body mass index in type 2 diabetic subjects. Tohoku J Exp Med 2005; 206: 23-30.

[62] Komiya Y, Katayama K, Yugi H, et al. Minimum infectious dose of hepatitis B virus in chimpanzees and difference in the dynamics of viremia between genotype A and genotype C. Transfusion 2008; 48: 286-94.

[63] Yatsuji H, Noguchi C, Hiraga N, et al. Emergence of a novel lamivudine-resistant hepatitis B virus variant with a substitution outside the YMDD motif. Antimicrob Agents Chemother 2006; 50: 3867-74.

[64] Tsuge M, Hiraga N, Akiyama R, et al. HBx protein is indispensable for development of viraemia in human hepatocyte chimeric mice. J Gen Virol 2010; 91: 1854-64.

[65] Sugiyama M, Tanaka Y, Kurbanov F, et al. Direct cytopathic effects of particular hepatitis B virus genotypes in severe combined immunodeficiency transgenic with urokinase-type plasminogen activator mouse with human hepatocytes. Gastroenterology 2009; 136: 652-62.

[66] Umehara T, Sudoh M, Yasui F, et al. Serine palmitoyltransferase inhibitor suppresses HCV replication in a mouse model. Biochem Biophys Res Commun 2006; 346: 67-73.

[67] Nakagawa S, Umehara T, Matsuda C, Kuge S, Sudoh M, Kohara M. Hsp90 inhibitors suppress HCV replication in replicon cells and humanized liver mice. Biochem Biophys Res Commun 2007; 353: 882-8.

[68] Inoue K, Umehara T, Ruegg UT, et al. Evaluation of a cyclophilin inhibitor in hepatitis C virus-infected chimeric mice in vivo. Hepatology 2007; 45: 921-8.

[69] Kamiya N, Iwao E, Hiraga N, et al. Practical evaluation of a mouse with chimeric human liver model for hepatitis C virus infection using an NS3-4A protease inhibitor. J Gen Virol 2010; 91: 1668-77.

[70] Ohara E, Hiraga N, Imamura M, et al. Elimination of hepatitis C virus by short term NS3-4A and NS5B inhibitor combination therapy in human hepatocyte chimeric mice. J Hepatol 2011; 54: 872-8.

[71] Takano T, Tsukiyama-Kohara K, Hayashi M, et al. Augmentation of DHCR24 expression by hepatitis C virus infection facilitates viral replication in hepatocytes. J Hepatol 2011; 55(3): 512-21.

[72] Katoh M, Matsui T, Okumura H, et al. Expression of human cytochrome P450 in chimeric mice with humanized liver. Drug Metab Dispos 2004; 32: 1402-10.

[73] Katoh M, Matsui T, Okumura H, et al. In vivo induction of human cytochrome P450 enzymes expressed in chimeric mice with humanized liver. Drug Metab Dispos 2005; 33: 754-63.

[74] Katoh M, Matsui T, Okumura H, et al. Expression of human phase II enzymes in chimeric mice with humanized liver. Drug Metab Dispos 2005; 33: 1333-40.

[75] Kitamura S, Nitta K, Tayama Y, et al. Aldehyde oxidase-catalyzed metabolism of N1-methylnicotinamide In vivo and In vitro in chimeric mice with humanized liver. Drug Metab Dispos 2008; 36: 1202-5.

[76] Katoh M, Sawada T, Soeno Y, et al. In vivo drug metabolism model for human cytochrome P450 enzyme using chimeric mice with humanized liver. J Pharm Sci 2007; 96: 428-37.

[77] Okumura H, Katoh M, Sawada T, et al. Humanization of excretory pathway in chimeric mice with humanized liver. Toxicol Sci 2007; 97: 533-8.

[78] Inoue T, Nitta K, Sugihara K, Horie T, Kitamura S, Ohta S. CYP2C9-catalyzed metabolism of S-warfarin to 7-hydroxywarfarin

In vivo and *In vitro* in chimeric mice with humanized liver. Drug Metab Dispos 2008; 36: 2429-33.

[79]   Inoue T, Nitta K, Sugihara K, Horie T, Kitamura S, Ohta S. Prediction of human disposition toward S-3H-warfarin using chimeric mice with humanized liver. Drug Metab. Pharmacokinet 2009; 24: 153-60.

[80]   Rettie AE, Korzekwa KR, Kunze KL, *et al.* Hydroxylation of warfarin by human cDNA-expressed cytochrome P-450: a role for P-4502C9 in the etiology of (S)-warfarin-drug interactions. Chem Res Toxicol 1992; 5: 54-9.

[81]   Yamasaki C, Kataoka M, Kato Y, *et al. In vitro* evaluation of cytochrome P450 and glucuronidation activities in hepatocytes isolated from liver-humanized mice. Drug Metab Pharmacokinet 2010; 25: 539-50.

[82]   Kamimura H, Nakada N, Suzuki K, *et al.* Assessment of chimeric mice with humanized liver as a tool for predicting circulating human metabolites. Drug Metab Pharmacokinet 2010; 25: 223-35.

Discrete Nature of EpCAM$^+$ and CD90$^+$ Cancer Stem Cells in Human Hepatocellular Carcinoma

Taro Yamashita,[1] Masao Honda,[1] Yasunari Nakamoto,[1] Masayo Baba,[1] Kouki Nio,[1] Yasumasa Hara,[1] Sha Sha Zeng,[1] Takehiro Hayashi,[1] Mitsumasa Kondo,[1] Hajime Takatori,[1] Tatsuya Yamashita,[1] Eishiro Mizukoshi,[1] Hiroko Ikeda,[1] Yoh Zen,[1] Hiroyuki Takamura,[1] Xin Wei Wang,[2] and Shuichi Kaneko[1]

Recent evidence suggests that hepatocellular carcinoma (HCC) is organized by a subset of cells with stem cell features (cancer stem cells; CSCs). CSCs are considered a pivotal target for the eradication of cancer, and liver CSCs have been identified by the use of various stem cell markers. However, little information is known about the expression patterns and characteristics of marker-positive CSCs, hampering the development of personalized CSC-targeted therapy. Here, we show that CSC markers EpCAM and CD90 are independently expressed in liver cancer. In primary HCC, EpCAM$^+$ and CD90$^+$ cells resided distinctively, and gene-expression analysis of sorted cells suggested that EpCAM$^+$ cells had features of epithelial cells, whereas CD90$^+$ cells had those of vascular endothelial cells. Clinicopathological analysis indicated that the presence of EpCAM$^+$ cells was associated with poorly differentiated morphology and high serum alpha-fetoprotein (AFP), whereas the presence of CD90$^+$ cells was associated with a high incidence of distant organ metastasis. Serial xenotransplantation of EpCAM$^+$/CD90$^+$ cells from primary HCCs in immune-deficient mice revealed rapid growth of EpCAM$^+$ cells in the subcutaneous lesion and a highly metastatic capacity of CD90$^+$ cells in the lung. In cell lines, CD90$^+$ cells showed abundant expression of c-Kit and *in vitro* chemosensitivity to imatinib mesylate. Furthermore, CD90$^+$ cells enhanced the motility of EpCAM$^+$ cells when cocultured *in vitro* through the activation of transforming growth factor beta (TGF-β) signaling, whereas imatinib mesylate suppressed *TGFB1* expression in CD90$^+$ cells as well as CD90$^+$ cell-induced motility of EpCAM$^+$ cells. *Conclusion*: Our data suggest the discrete nature and potential interaction of EpCAM$^+$ and CD90$^+$ CSCs with specific gene-expression patterns and chemosensitivity to molecular targeted therapy. The presence of distinct CSCs may determine the clinical outcome of HCC. (HEPATOLOGY 2012;00:000–000)

The cancer stem cell (CSC) hypothesis, which suggests that a subset of cells bearing stem-cell–like features is indispensable for tumor development, has recently been put forward subsequent to advances in molecular and stem cell biology. Liver cancer, including hepatocellular carci-noma (HCC), is a leading cause of cancer death worldwide.[1] Recent studies have shown the existence of CSCs in liver cancer cell lines and primary HCC specimens using various stem cell markers.[2-7] Inde-pendently, we have identified novel HCC subtypes defined by the hepatic stem/progenitor cell markers,

1

epithelial cell adhesion molecule (EpCAM) and alpha-fetoprotein (AFP), which correlate with distinct gene-expression signatures and prognosis.[8,9] EpCAM^{+} HCC cells isolated from primary HCC and cell lines show CSC features, including tumorigenicity, invasiveness, and resistance to fluorouracil (5-FU).[10] Similarly, other groups have shown that CD133^{+}, CD90^{+}, and CD13^{+} HCC cells are also CSCs, and that EpCAM, CD90, and CD133 are the only markers confirmed to enrich CSCs from primary HCCs thus far.[3-5,10]

Although EpCAM^{+}, CD90^{+}, and CD133^{+} cells show CSC features, such as high tumorigenicity, an invasive nature, and resistance to chemo- and radiation therapy, it remains unclear whether these cells represent an identical HCC population and whether they share similar or distinct characteristics. In this study, we used fluorescent-activated cell sorting (FACS), microarray, and immunohistochemistry (IHC) techniques to investigate the expression patterns of the representative liver CSC markers CD133, CD90, and EpCAM in a total of 340 HCC cases and 7 cases of mesenchymal liver tumors. We further explored gene- and protein-expression patterns as well as tumorigenic capacity of sorted cells isolated from 15 primary HCCs and 7 liver cancer cell lines in an attempt to identify the molecular portraits of each cell type.

Materials and Methods

Clinical Specimens. HCC samples were obtained with informed consent from patients who had undergone radical resection at the Liver Center in Kanazawa University Hospital (Kanazawa, Japan), and tissue acquisition procedures were approved by the ethics committee of Kanazawa University. A total of 102 formalin-fixed and paraffin-embedded HCC samples, obtained from 2001 to 2007, were used for IHC analyses. Fifteen fresh HCC samples were obtained between 2008 and 2012 from surgically resected specimens and an autopsy specimen and were used immediately to prepare single-cell suspensions and xenotransplantation (Table 1). Seven hepatic stromal tumors (three cavernous hemangioma, two hemangioendothelioma, and two angiomyolipoma) were formalin fixed and paraffin embedded and used for IHC analyses.

Table 1. Clinicopathological Characteristics of HCC Cases Used for Xenotransplantation

ID	Age/Sex	Etiology	Tumor Size (cm)	Histological Grade	AFP (ng/mL)	DCP (IU/mL)
P1	77/M	Alcohol	12.0	Moderate	198	322
P2	61/F	NBNC	11.0	Moderate	12	3,291
P3	66/M	NBNC	2.2	Moderate	13	45
P4	65/M	HCV	4.2	Poor	13,700	25,977
P5	52/M	HBV	6.0	Moderate	29,830	1,177
P6	60/M	HCV	2.7	Poor	249	185
P7	79/F	HBV	4.0	Poor	46,410	384
P8	77/F	NBNC	5.5	Moderate	17,590	562
P9	71/M	Alcohol	7.0	Poor	3,814	607
P10	51/M	HBV	2.2	Well	<10	21
P11	71/M	Alcohol	2.1	Well	<10	11
P12	60/M	HBV	10.8	Poor	323	2,359
P13	66/M	HCV	2.8	Moderate	11	29
P14	71/M	HCV	7.2	Moderate	235,700	375,080
P15	75/M	HBV	5.5	Poor	<10	97

Abbreviation: DCP, des-gamma-carboxy prothrombin.

Additional details of experimental procedures are available in the Supporting Information.

Results

EpCAM, CD133, and CD90 Expression in HCC. We first evaluated the frequencies of three representative CSC markers (EpCAM^{+}, CD90^{+}, and CD133^{+} cells) in 12 fresh primary HCC cases surgically resected by FACS (representative data shown in Fig. 1A). Clinicopathological characteristics of primary HCC cases are shown in Table 1. We noted that frequency of EpCAM^{+}, CD90^{+}, and CD133^{+} cells varied between individuals. Abundant CD90^{+} (7.0%), but almost no EpCAM^{+}, cells (0.06%, comparable to the isotype control) were detected in P2, whereas few CD90^{+} (0.6%), but abundant EpCAM^{+}, cells (17.5%) were detected in P4. Very small populations of EpCAM^{+} (0.09%), CD90^{+} (0.04%), and CD133^{+} cells (0.05%) were found in P12, but they were almost nonexistent in P8, except for CD90^{+} cells (0.08%) (Fig. 1A). We further evaluated the expression of EpCAM, CD90, and CD133 in xenografts obtained from surgically resected samples (P13 and P15) and an autopsy sample (P14). As a whole, compared to the isotype control, 7 of 15 HCCs contained definite EpCAM^{+} cells (46.7%), whereas only 3 HCCs